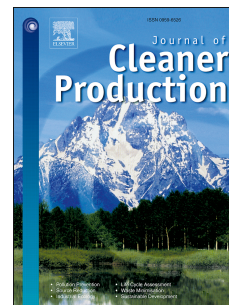


Journal Pre-proof

Mitigation Strategy of Carbon Dioxide Emissions through Multiple Muffler design exchange and Gasoline-Methanol blend replacement

Prakash Chandra Mishra, Rihana.B. Ishaq, Fuad Khoshnaw



PII: S0959-6526(20)35506-2

DOI: <https://doi.org/10.1016/j.jclepro.2020.125460>

Reference: JCLP 125460

To appear in: *Journal of Cleaner Production*

Received Date: 27 September 2020

Revised Date: 3 November 2020

Accepted Date: 7 December 2020

Please cite this article as: Chandra Mishra P, Ishaq RB, Khoshnaw F, Mitigation Strategy of Carbon Dioxide Emissions through Multiple Muffler design exchange and Gasoline-Methanol blend replacement, *Journal of Cleaner Production*, <https://doi.org/10.1016/j.jclepro.2020.125460>.

This is a PDF file of an article that has undergone enhancements after acceptance, such as the addition of a cover page and metadata, and formatting for readability, but it is not yet the definitive version of record. This version will undergo additional copyediting, typesetting and review before it is published in its final form, but we are providing this version to give early visibility of the article. Please note that, during the production process, errors may be discovered which could affect the content, and all legal disclaimers that apply to the journal pertain.

© 2020 Elsevier Ltd. All rights reserved.

CRediT authorship contribution statement

PC Mishra: Conceptualization, write-up, Experimentation, CFD analysis and CAD Modelling and computation.

RB Ishaq: Conceptualization, writing and verification. **F Khoshnaw:** Conceptualization, writing and verification.

Mitigation Strategy of Carbon Dioxide Emissions through Multiple Muffler design exchange and Gasoline-Methanol blend replacement

Prakash Chandra Mishra^{a,b}, Rihana B. Ishaq^c Fuad Khoshnaw^d

^a*Department of Mechanical Engineering, Veer Surendra Sai University of Technology, Burla, India-768018*

^c*School of Engineering, Technology and Design, Canterbury Christ Church University, Kent, UK*

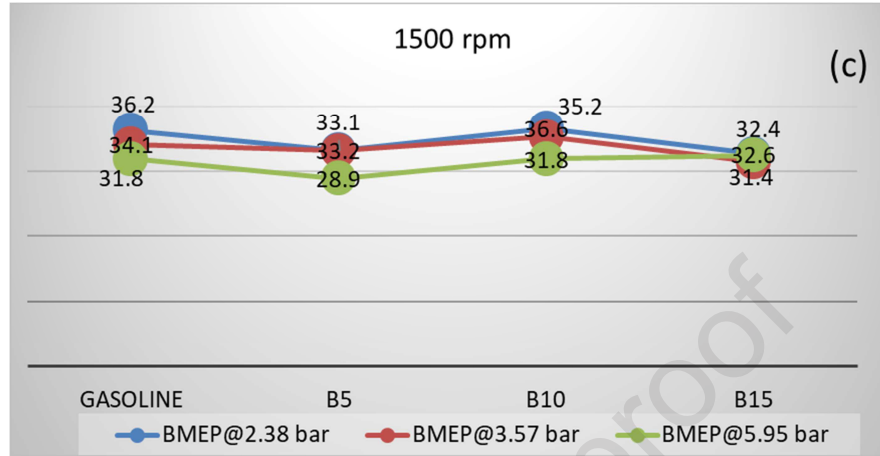
^d*School of Engineering and Sustainable Development, De Montfort University, Leicester, UK*

^bCorresponding author:

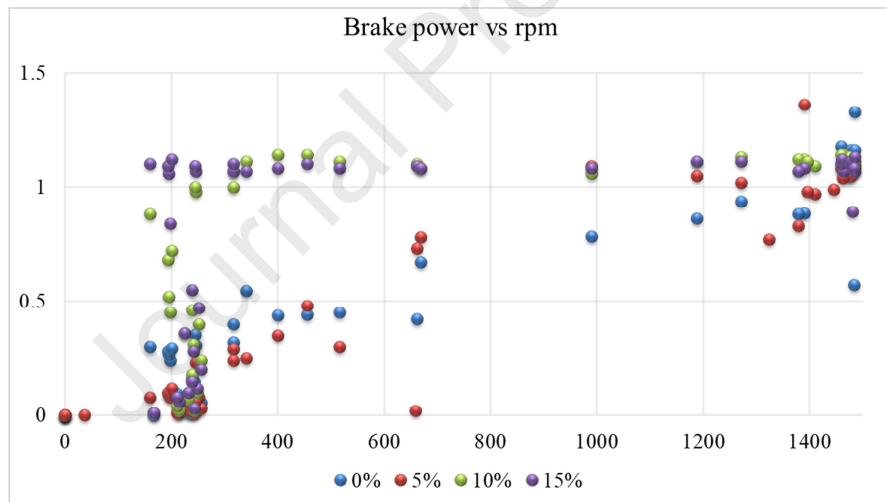
Dr Prakash Chandra Mishra
Associate Professor
Department of Mechanical Engineering
Veer Surendra Sai University of Technology
Burla, Odisha
Pin-768017, India
Mobile-+918917535445

Email: pcmishra_me@vssut.ac.in

Mitigation Strategy of Carbon Dioxide Emissions through Multiple Muffler design exchange and Gasoline-Methanol blend replacement



(a) CO₂ response to Gasoline-Methanol blend (Variable BMEP)



(b) Brake power response to rpm for different fuel replacement

Mitigation Strategy of Carbon Dioxide Emissions through Multiple Muffler design exchange and Gasoline-Methanol blend replacement

Prakash Chandra Mishra^{a,b}, Rihana B. Ishaq^c Fuad Khoshnaw^d

^aDepartment of Mechanical Engineering, Veer Surendra Sai University of Technology, Burla, India-768018

^cSchool of Engineering, Technology and Design, Canterbury Christ Church University, Kent, UK

^dSchool of Engineering and Sustainable Development, De Montfort University, Leicester, UK

^bCorresponding author:

Dr Prakash Chandra Mishra
Associate Professor
Department of Mechanical Engineering
Veer Surendra Sai University of Technology
Burla, Odisha
Pin-768017, India
Mobile:+918917535445

Email: pcmishra_me@vssut.ac.in

Research Highlights

- Need for blending Methanol-Gasoline to test and compare CO₂ emissions.
- Conduct Engine testing to carry out emissions and performance study.
- Mitigation strategy of CO₂ emissions through four-muffler design replacements.
- Sustainability of integrating fuel-blend and exhaust muffler design in CO₂ reduction.

Abstract:

Use of fuel blend in place of traditionally used fossil fuel, significantly reduced carbonated emissions from internal combustion engine. Further reduction of such emissions with controlled 'NO_x yield' is a challenge faced by researchers. Modification of muffler geometry in an engine while using blended fuel, helps reduction of muffler temperature and subsequently diminish NO_x formation and alters CO₂ emissions. This paper investigates a hybrid method to mitigate the CO₂ emissions from SI engines, through use of gasoline-methanol blend with 5%, 10% and 15% of methanol by volume. Moreover, along with this, four different design mufflers are tried for testing to see their effect on CO₂ emissions. In this frame work comprehensive tests were carried out to measure CO₂ emissions from a single cylinder 4-stroke SI engine operating in different combinations of brake mean effective pressure; 2.38 bar, 3.57 bar, 5.95 bar and speeds; 500 rpm,

1000 rpm and 1500 rpm. The results depict that chambered type non-perforated muffler (Type-A) is best among all designs for reducing CO₂ emissions. While, turbo perforated (Type-D) muffler has most CO₂ emissions compared to all designs. The effect of perforation on CO₂ emissions is maximum at BMEP@3.57 bar for turbo type muffler.

Keywords: Emission reduction strategy; CO₂ mitigation; Gasoline-Methanol blend; Chamber-Muffler; Turbo-Muffler

1. Introduction

Carbon dioxide (CO₂) emissions are one of the major constituents of greenhouse gases, mainly generated from vehicles that are major sources of CO₂ (Aye et al., 2017). A rapid increase in the use of automobiles, powered by fossil fuels, emit CO₂, CO, NO_x and HC on a large scale to the environment. Urban areas are more prone to environmental degradation compared to rural ones due to increased vehicle density. This creates an imbalance of atmospheric constituents, leading to a health hazard among people (Ekwurzel et al., 2017). Large cities like London, Delhi, Shanghai, Tokyo, etc. have already passed through the phase of the dangerous effects of CO₂ emissions (Terrenoire et al., 2007). Society is so dependent on vehicles that it is difficult to consider an alternative way of moving around, which can have less CO₂ emissions compared to automotive.

Alternative power systems that produce less CO₂ emissions, such as electric vehicles and hybrid technologies for vehicles are being developed, but their current cost and the supportive infrastructure is prohibitive for most cities (Office of low carbon vehicle U.K, 2013). Even well-developed economies are introducing these at a slow and steady pace to enable technology to be established. In the UK, the overall carbon target largely decarbonized road transport sector by

2050. To achieve this from 2040 onwards every single vehicle to be sold to be ultra-low emission vehicles (Office of low carbon vehicle U.K, 2013).



Fig.1 World Carbon dioxide emission levels (<http://lert.co.nz/map>)

Fig.1 shows the global carbon dioxide emission distribution. In terms of CO₂ emission, the United States of America and China remain the major contributor followed by Australia, Canada, India, Russia and Brazil. Advanced combustion concept combined with alternate fuel is a way to improve engine-out emission and efficiency, need to be improved considering the state of the art of most recent technologies in the field of IC engines. In this context, replacement of fossil fuel with bio-fuel blend significantly reduced the carbonated emissions without any compromise on efficiency and performance (Vassallo et al., 2018; Blasio et al., 2020). One such example is gasoline replaced with gasoline-methanol blend, that improved combustion of air-fuel mixture, due to which, the exhaust gas temperature also enhanced. This condition is conducive for aggravated NO_x formation. Many attempts such as EGR valve and catalytic converter provision help reducing the heat in exhaust system, modification of muffler design and it's effect on surface temperature distribution will be also worth of observation.

2. Background Motivation

Increases in atmospheric temperatures and rising sea levels are the indicators of a heavy presence of CO₂ in the atmosphere (Ekwurzel et al., 2017). (Terrenoire et al., 2007) carried out anthropogenic CO₂ emission recording for 343 cities. Here data from individual cities are subject to quality control to separate from those of other greenhouse gases. Through this analysis, some set of ancillary data from other sources (socio-economic and traffic indices) or calculated (climate indices, urban area expansion) and combined with emission data. (Aye et al., 2017) studied the effect of economic growth (EG) on CO₂ emission using a dynamic panel threshold framework. The results show the EG has a negligible effect on CO₂ emissions. There is evidence of a significant causal relationship between CO₂ emission, economic growth, energy consumption and financial development. The findings emphasize the need for the transformation of low carbon technologies aimed at reducing emissions and sustainable economic growth. This may include energy efficiency and switching away from non-renewable energy to renewable energy. (Abeydeer et al., 2019) identified sulphur dioxide, nitrogen dioxide and carbon dioxide as prime causes of global climate change. Out of them, CO₂ is recognized as a good agent for exploring the strategy for carbon reduction and mitigation.

(Valihesari et al., 2019) tested a blend of gasoline, oxygenate additive; methanol and metal nanoparticles: Fe₂O₃ and TiO₂ in a 4-stroke engine to investigate the effects of the new blend on the engine parameters, such as power and torque and also the amount of target pollutant gases emitted which are CO₂, CO, NO_x and HC. The research being undertaken, around the world, is now mainly focusing on reducing engine emissions while using fossil fuels. (Verhelst et al., 2019) reviewed the use of methanol as a pure fuel or blend component for ICEs. They summarized various method of methanol production and also the health and safety issues

associated with the use of methanol as a fuel for ICEs. Many properties of methanol (for example high heat of vaporization) are superior to that of gasoline. This helps make blended fuels a suitable improved alternative to traditional automotive fuel compositions. It is necessary to address changes in hardware, materials and heat recovery to improve the engine efficiency when using methanol. Furthermore, the behaviour of methanol fuel such as, mixture formation, normal/abnormal combustion, high latent heat, fast-burning velocity, high knock resistance, etc. are reviewed for the modelling aspect. Blended fuels show promising performance as compared to traditional gasoline or diesel fuel. (Shrivastava et al., 2019) through transesterification of a bio-diesel from Karanja and Roselle oil, tested for emissions and performance. They achieved lower thermal efficiency with a reduction of exhaust gas temperature by 1.48% and 1.38%. However, brake specific fuel consumption increased by 4.13% compared to traditional diesel fuel. Also, the use of blend shows 15.3% less NO_x and 1.92% more CO_2 compared to diesel. Through this analysis, an artificial neural network (ANN) model was developed to predict the output parameter through a multivariable response.

(Athanasopoulou et al., 2018; Lijewski et al., 2019) studied a plug-in hybrid electric vehicle (PHEV) and Battery Electric Vehicle (BEV) considering combustion engine as a range extender and compared CO, THC and NO_x for urban (route-1) and extra-urban (route-2). In both cases, PHEV engine yields HC less by 69%, 6%; CO less by 69%, 80% respectively. It was suggested BEV not to be used in battery only mode, which lead to activation of range extender and more emission report. (Çelik, M., & Bayindirli, 2019) considered blending of rapeseed methyl ester with n-hexane and n-hexadecane to examine its effect on engine emissions (HC, CO, PM). Such fuel modification improved BTE and HRR both. It is observed that HC, CO and soot formation decreased significantly, while NO_x increases 2.262% and 3.2% respectively.

(Mourad et al., 2019) studied the blending of gasoline-ethanol and gasoline-butanol (25,5%,10%,15%) on the emissions and power of an engine. They observed a 13.7% reduction in CO₂, 25.2% reduction in hydrocarbon, 8.22% reduction in fuel consumption. However, they also reported an 11.1% reduction in engine power. (Blasio et al., 2017; Beatrice et al., 2017) carried out experimental investigations to understand the functional requirements to achieve 100 kW/l in high speed light duty diesel engines. In order to achieve this, a high-performance prototype was employed with advanced piezo-injection system with 3000 bar pressure, which confirmed benefits of high fuel injection pressure on performance as well as fuel economy of light-duty diesel engine. (Vassallo et al., 2018; Blasio et al., 2020) investigated the effect of balance between fuel injection parameter and hydraulic flow (HF) in achieving low-emission and enhanced efficiency in diesel engines. Such study monitored performance, efficiency and noise simultaneously using a 0.5 dm³ single-cylinder diesel engine and predicted the optimized combination of HF and injection options. Recent trends of Diesel engine development is shifting from performance to ultra-low emissions along with improved efficiency. Further to the analysis of ultra-low emission achievement, (Belgiorno et al., 2020) developed additive manufacturing-enabled diesel combustion bowl for optimized combustion phenomena. Through a 2500 bar fuel injection pressure, the fuel air mixing improvement was confirmed, which enhanced completeness in combustion.

Due to the uncontrolled use of vehicles operating on fossil fuels, regulations are defined to curb emission levels at a regional or countrywide level. (Olabi et al., 2020) reviewed the regulations and techniques to eliminate toxic emissions from diesel engine cars. (Rao et al., 2018) carried out a review on the performance of the IC engine using alternative fuels. An attempt was made to

design and develop IC engine parts that are most suitable for alternate fuels, that can last longer without affecting the performance of the engine.

Numerous studies were carried out on exhaust muffler in understanding the noise and acoustic emissions from engine outlet and suggestions implemented to improve noise quality through various methods (Hasimoto et al., 2013; Inoue et al., 2003). (Reddy, 2016) carried out a review on various acoustic methods and material selection for muffler used in automobile, aerospace and industrial compressor applications. Parameters such as stress, temperature, thermal conductivity and gas density were reviewed for different materials for muffler applications. They discussed the effect of material porosity, metallic substrate pattern and ceramic substrate pattern on acoustic performance of exhaust muffler. (Ramasso et al., 2020) developed computational technique to detect, develop, constraint-based consensus clustering technique to interpret acoustic emission stream originating from composite material. But such studies limited to acoustic characteristics and noise refinement. Very limited researches put forward to discuss the effect of muffler design on exhaust emission performance of ICEs.

(Mishra et al., 2020; Gupta et al., 2019) aimed to fully evaluate the effects of petrol-methanol blends on the emission and performance of engines and the corresponding noise levels. Petrol blended with 5%, 10% and 15% of methanol was used in three separate tests, which are conducted at constant torque and variable speed conditions. The exhaust emission analysis was done using six gas emissions analyzer. The emission levels were measured, while the engine was mounted in a special purpose engine testbed fitted with an eddy current dynamometer capable of controlling the speed and torque of the engine. The noise level of the silencer was also measured to understand the effects of methanol percentage on engine knock. The analysis predicts the blend of 5%, 10% and 15% methanol with gasoline exhibited fewer emissions and knocking

behaviour compared to pure petrol. In some cases, the NO_x emissions of richer fuel blends were higher than that of leaner ones. However, other emission constituents were significantly reduced when using the methanol blend in place of pure petrol.

Based on this broad literature review, it is understood that most of the research concentrated on the use of blending, while few of them reported modelling and simulation. Very few reported the cumulative effect of fuel blends and engine modification on emissions, especially CO_2 and its reduction and mitigation strategy.

One of the promising methods is to replace traditional fuel (gasoline/ diesel) with fuels that have been blended with lighter components. The objective of this work is to adopt the fuel variation in the engine through replacements of Gasoline with B₅, B₁₀ and B₁₅. Also, to implement muffler design modification for monitoring the trend of CO_2 in an SI engine. The key findings of this study will be beneficial for the policymakers, academics, and institutions to determine the future research directions as well as to identify with whom they can consult to assist in developing carbon emission control policies and future carbon reduction targets.

2. Materials and Methods

Different techniques are considered to achieve a reduction and mitigation of CO_2 in an ICE. One such technique is to replace pure gasoline with a gasoline-methanol blend. It is not possible to operate the engine with pure methanol as the fuel is hugely toxic and burns with an invisible flame. Furthermore, pure methanol is very corrosive to the engine components and reduce the working life significantly compared to gasoline. To manage these negative effects, the methanol percentage is maintained at low levels of 5%, 10% and 15% respectively.

2.1 Gasoline-Methanol blend preparation and characterization

The composition of the blend in this study is made to (95% by vol. of Gasoline and 5% by vol. of Methanol) B₅, (90% by vol. of Gasoline and 10% by vol. of Methanol) B₁₀ and (85% by vol. of Gasoline and 15% by vol. of Methanol) B₁₅. The reason for choosing this composition is that there is no significant variation in fuel characteristics, especially health and safety related toxicity is not much different to gasoline. Option for higher gasoline % in blend is not good for engine metallic components, due to possibility of corrosion effect. The blending is done manually and is effective due to the high diffusivity of methanol in gasoline.

The comparative values of different parameters are calculated based on the following equations.

The density of the blend of two liquids were numerically computed as per equation (1)

$$\rho_{blend} = \frac{\rho_g V_g + \rho_m V_m}{V_g + V_m} \quad (1)$$

Kinematic viscosity for the blend were estimated numerically using three different methods; Gambill method (Gambill et al., 1959), Refuta equation and Chevron formula as given in Eq. (2), Eq (3) and Eq (5) respectively.

$$\kappa_{blend} = x_g \kappa_g^{\frac{1}{3}} + x_m \kappa_m^{\frac{1}{3}} \quad (2)$$

As per (Maples et al., 2000), Refuta-mass fraction basis yields

$$VBN_i = 14.534 \times \ln(\ln(\kappa_i + 0.8)) + 10.975 \quad (3)$$

$$VBN_{blend} = \sum_{i=0}^{n=0} x_i VBN_i \quad (4)$$

$$\kappa_{blend} = \exp \left(\exp \left(\frac{VBN_{blend} - 10.975}{14,534} \right) \right) - 0.8 \quad (5)$$

Chevron formula (volumetric basis)

$$VBN_i = \frac{\ln(\kappa_i)}{\ln(1000 \times \kappa_i)} \quad (6)$$

$$VBN_{blend} = \sum_{i=0}^{n=0} v_i VBN_i \quad (7)$$

The octane number of a blend is calculated on basis of the formula given in Eq. (8)

$$OCT_{blend} = OCT_{gasoline} \times (v_{gasoline}) + OCT_{methanol} \times (v_{methanol}) \quad (8)$$

Once the blends were ready, the fuel characteristics of the blends were studied with particular focus on how those desired properties were comparable to the pure gasoline which was to be replaced. Table 1 shows the comparative value of B₅, B₁₀ and B₁₅ with gasoline and methanol.

Table 1 Comparative values of blend for gasoline and methanol

<i>Fuel properties</i>	<i>Testing standard</i>	<i>Gasoline</i>	<i>B5</i>	<i>B10</i>	<i>B15</i>	<i>Methanol</i>
Density (kg/m ³)	ASTM 4052	780	780.6	781.2	781.8	792
Kinematic viscosity (C Stoke)	ASTM D445	0.88	0.87	0.857	0.845	0.65
Acid value (mg KOH/g)	ASTM D664	0.32	0.30	0.295	0.29	0.45
Flashpoint (°C)	ASTM D93	-43	-40.4	-37.8	-35.2	9
Calorific value (kJ/kg)	ASTM D240	47300	46670	44840	43610	22700
Auto-ignition temperature (°C)	ASTM E659	580	572	564	556	420
Octane number	ASTM D2700 (MON)	92	94	95.8	97.7	130
	ASTM D2699 (RON)	100	100.1	100.2	100.3	102

2.2 Material for muffler manufacturing

Though muffler design has significant effect on exhaust efficiency, the modification of fluid path and re-design of chamber volume may have significant effect in emission control, that we wish to know through this research work. As such reformation directly modify the chamber temperature, velocity streamline etc. This attempt may have significant impact on pumping loss, that we wish to figure out through back pressure analysis. Hence, Muffler design modification, is one of the CO₂ mitigation techniques, which was considered in this study. The mufflers were manufactured out of GI pipes and sheets ($E=200GPa$, $\nu=0.29$). The fabrication process includes metal sheet forming, welding, hole drilling and assembly. All the activities are performed in the Central Workshop of KIIT University Bhubaneswar. Fig. 2 shows the four different mufflers prepared for this analysis. The chamber non-perforated muffler has baffle plates, while perforated one is having holes in the angular baffle plates. Similarly, turbo non-perforate and turbo perforated are having pipes, whereas the later one is having perforation in pipes.

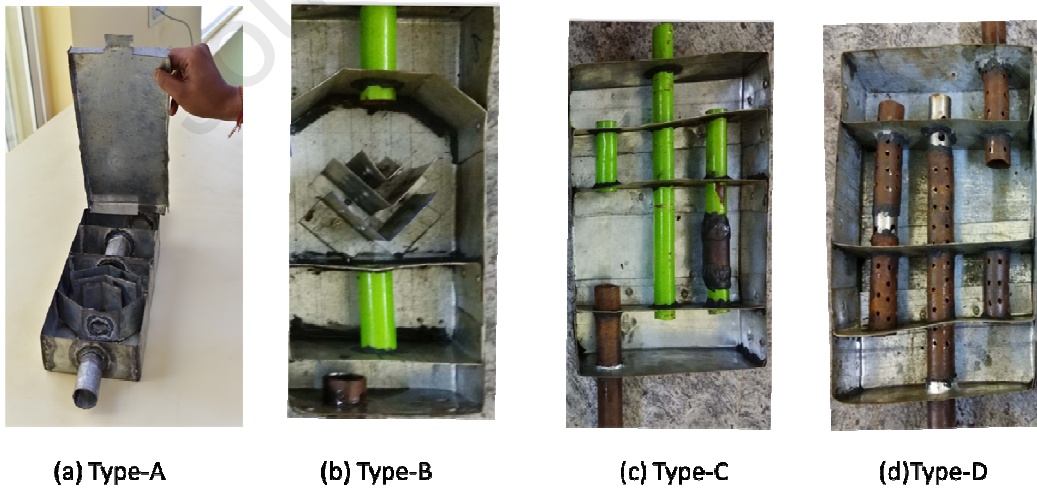


Fig. 2 Muffler manufacturing, (a) Type A: Chamber non-perforated, (b) Type B: Chamber perforated, (c) Type C: Turbo non-perforated and (d) Type D: turbo perforated

Though the emission absorbent filter in the mufflers, the EGR valve and the catalytic converter are the main components in the exhaust system that are responsible for reducing the generated emissions from the engine, a simple model of muffler is advisable to use in the design stage, which yield comparatively more emission in bared state, even more reduction is possible in fully loaded condition once such attachments are inserted.

Fig. 3 a-b show the fluid content of chamber type and turbo type muffler respectively, which will be later considered for the modeling of flow behavior and heat dissipation phenomena. Fig. 3(c-d) depicts the axial streamline of flow trajectory of two muffler designs. The path in the previous case is streamline, while the latter one is feedback type. In the second case, the backpressure is more.

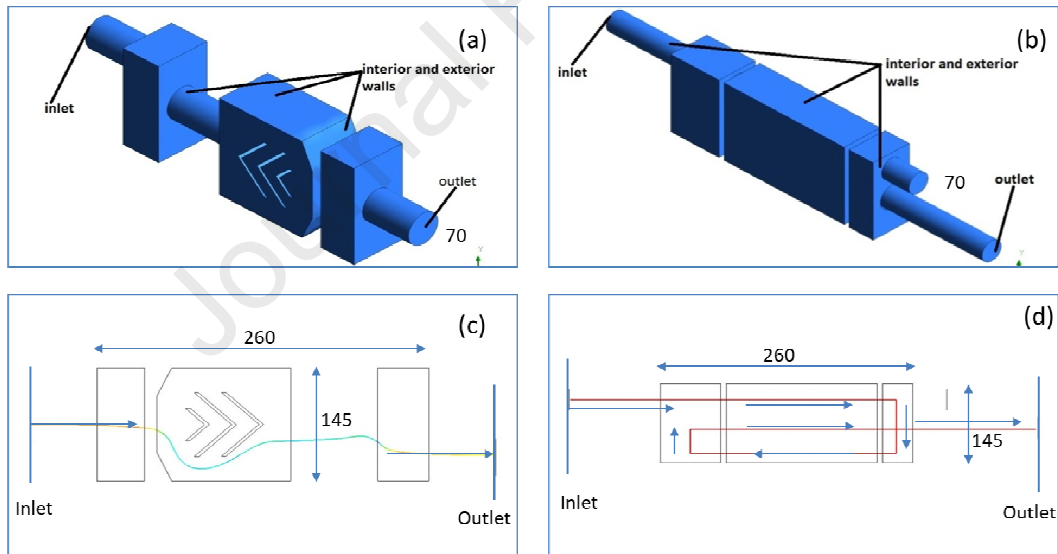


Fig.3 Exhaust gas path (Mishra et al., 2020) in, a: Chamber type muffler fluid content, b: Turbo type muffler fluid content, c: Evaluated fluid path-chambered type and d: Evaluated fluid path-turbo type

2.3 Engine-Testbed-Emission Analyzer

Four-stroke, single-cylinder, double valve, 105.6 cc engine (Mishra et al., 2020) was used in this study. The bore to stroke dimension equals 49.0x56.0 mm, a compression ratio is 9:1, and can

deliver power maximum up to 6 kW with 7500 rpm. It has the provision of wet-sump lubrication, air cooling and used wet type multi-plate clutch. It is fitted with a four-speed constant mesh type gear transmission system. Figure 4(d) shows the engine of this specification mounted in the test bed for testing.

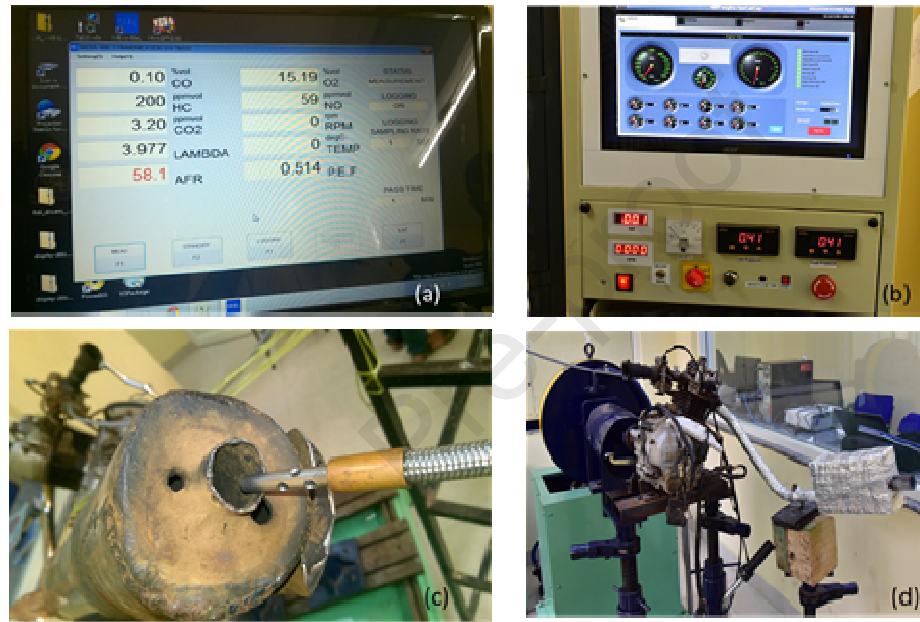


Fig.4 Emission measurement, a: Emission data acquisition, b: performance data acquisition, c: emission sensing at the exhaust and d: engine testbed

Table 2 shows the specification of the dynamometer for this study. The dynamometer used here is eddy current type with maximum engine torque of 90 Nm and 7000 rpm. APPSYS WED 38S type magnetic water strainer is used here along with a water flow switch, reaction type torque sensor, torque calibration arm and magnetic pickup sensor. The control panel is equipped with PC hardware, PCI data card and a data acquisition system to view and control the torque (N.m), speed (rpm), mechanical power (kW/HP), pressure (N/m^2) and temperature ($^{\circ}\text{C}$). Data acquired was stored in an excel sheet along with various graphical outputs. The dynamometer was controlled either in automatic mode or manual mode.

258 **Table 2** Specification of water-cooled Eddy current dynamometer with 38 kW power rating (Mishra et al., 2020)

Attributes	Details
Model	APPSYS WED 38S
Rated absorption Power (kW)	38 kW (50 hp).
Maximum torque (Nm)	90 Nm
Maximum Torque at Speed Range	1400 to 4031 rpm
Maximum Speed (R / Min)	7000 rpm (for Speed more than 7000 rpm high-speed bearings are used.)
Torque measurement precision (F. S.)	± 0.5 FS%, 0.1 Nm resolution
Speed measurement precision (F. S.)	± 0.5 FS %, 1 rpm resolution
The direction of rotation	Both Direction, Clockwise and Anti-Clock wise
Max. Water Flow (Ltrs / hr) with Pressure	1400 Ltrs/hr at 1 – 2 bar pressure
Drainage maximum temperature (°C)	65
Moment of inertia (kgm ²)	0.018

259

260 2.4 Emission measurement using HORIBA MEXA-584L Emission Analyzer

261 The emission analyzer used in this study was the HORIBA make MEXA-584L, which can
 262 simultaneously sense CO, HC and CO₂ using the non-dispersive infrared (NDIR) technique. The
 263 air-to-fuel-ratio or excess air ratio (A) was measured with this analyzer. The analyzer is a mobile
 264 system, which can even be used outdoors and has a single screen. Also, O₂, NO_x, engine speed
 265 and oil temperature were measured in this instrument. Table 3 provides the detailed
 266 specifications of the emission analyzer.

267

268

269

270 **Table 3** Specification of Horiba Mexa 584-L emission gas analyzer (Mishra et al., 2020)

<i>Attributes</i>	<i>Details</i>
Measured gas components (standard)	<ul style="list-style-type: none"> CO, CO₂, LAMBDA (Unburnt HC), O₂ and NO_x
Measuring principle	<ul style="list-style-type: none"> CO, HC, CO₂: Non-dispersive infrared (NDIR) Air-to-fuel ratio (AFR), Lambda: Carbon balance method, or Brettschneider method with O₂ measurement. AFR and lambda are calculated by carbon balance in standard configuration.
Conformed standard	<ul style="list-style-type: none"> OIML Class 0-CE-FCC.
Ambient humidity	<ul style="list-style-type: none"> Under 90% relative humidity.

271

272 Fig. 4a shows this emission analyzer in action, measuring exhaust gases from the engine. It
 273 should be ensured that the source of power is stable. Before switching on the analyzer, it is
 274 ensured that the sensing pipe end is made leak-proof using a rubber cap. After a warmup period
 275 of 300s, it automatically starts the leak detection test. If it fails the leak detection test, the leak
 276 proofing should be inspected and the procedure is repeated. If it passes the leak detection test, the
 277 measuring of HC following the removal of the cap can be undertaken. Once the HC hang-up test
 278 was done, the analyzer is ready to measure the emissions from the engine. There is one
 279 communication software in MEXA-584L, which can interface the machine with the computer
 280 with a sampling rate and sampling time. The data can be recorded once every 3s for 120s and
 281 stored in an excel sheet.

282 2.5 CO₂ Emission formation mechanism

283 There are three types of emission formed in a running engine; exhaust emissions, crankcase
 284 emissions and evaporative emissions. In this analysis, we considered the exhaust emissions. As

per earlier studies (Gupta et al., 2019), 100 % CO/CO₂ emissions are from the exhaust of combustion gases. The emissions formation mechanism of CO₂ is a two-step process (NPTEL IITK, 2012). The first step is the conversion of HC to CO, where several oxidation reactions are involved in the formation of intermediate compounds like small HC molecules, aldehyde, ketones, etc. based on equation (1)



With the availability of sufficient oxygen in air conversion of CO to CO₂ is ensured. The chemical reaction is given in equation (2). The formation of CO₂ is the reassurance that complete combustion has occurred and sufficient oxygen and time were available to eliminate unburned HC from the exhaust gases. However, the quantity of CO₂ is directly related to the performance of the engine. The trend in modern engines is to reduce fuel consumption and thus reduce the CO₂ emissions by reducing fuel consumption, improving combustion processes and reducing the overall engine mass and friction through improved engine refinement.



2.6 CO₂ Emission Measurement

In this study, a single-cylinder spark-ignition engine was implemented, the details are shown in Fig 4(d). The engine was operated at different combinations of torque and speed to acquire the CO₂ emissions. A load calibration test was carried out by applying 10 kg weight. As the load arm is 50 cm, the torque monitor should show 49 Nm torque reading on both the left and right sides of the arms as shown in Fig. 5. It was carried out to ensure that the digital as well as

computerized data acquisition systems are accurate. Continuous water circulation into the eddy current dynamometer is ensured by an external pump arrangement to extract the frictional heat out of the dynamometer due to engine braking. Such monitoring is done by observing the green color of the indicator light provided in the data acquisition monitor for dynamometer water supply.

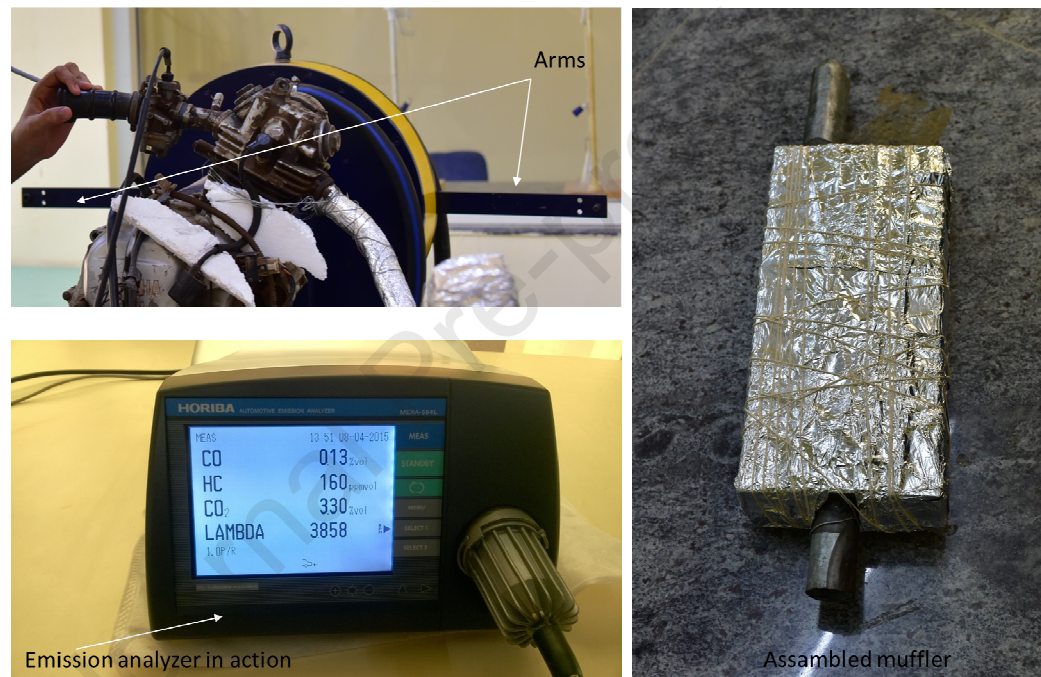


Fig. 5 Dynamometer arm, emission analyzer in measuring mode and assembled muffler

3. Results and Discussion

3.1 Emission Analysis Results and Discussion

Fig. 6(a-d) show CO_2 response to engine BMEP (2.38 bar, 3.57 bar and 5.95 bar) at 500 rpm. In all cases (Gasoline, B₅, B₁₀ and B₁₅) chambered type muffler (Type-A and Type-B) shows less CO_2 emission compared to turbo type muffler (Type-C and Type-D). Chambered type non-perforated muffler (Type-A) has the lowest (15.57 gm/kWh) amount of CO_2 emissions from pure

gasoline fuel at BMEP@2.38 bar. The turbo perforated (Type-D) muffler has the highest CO₂ emissions (53.72 gm/kWh). Perforation led to a 42% increase in CO₂ for all chambered type mufflers at BMEP@2.38 bar and BMEP@5.95 bar, while using gasoline at 500 rpm. The effect of perforation in the chambered type muffler shows less difference in CO₂ emission at 500 rpm. For the turbo type muffler, running on pure gasoline fuel the difference is less, but for blended fuels (B₅, B₁₀ and B₁₅) larger differences of CO₂ emissions are observed, and more so in the case of the perforated turbo type (Type-D). The chambered type mufflers have almost half the level of CO₂ emissions as compared to turbo mufflers.

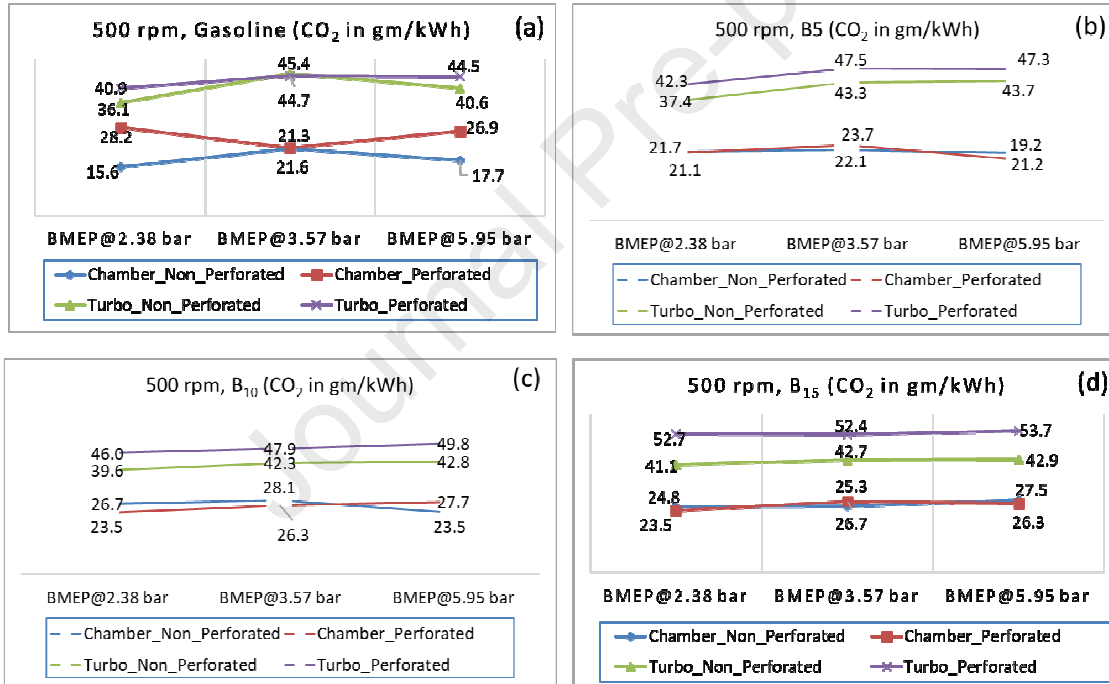


Fig.6 CO₂ response to engine BMEP, (a) Gasoline at 500 rpm, (b) B₅ at 500 rpm, (c) B₁₀ at 500 rpm and (d) B₁₅ at 500 rpm

Figs. 7(a-d) show the CO₂ response to engine BMEP (2.38 bar, 3.57 bar and 5.95 bar) at 1000 rpm. As the speed increases from 500 rpm to 1500 rpm, the CO₂ emissions increase in all cases. The lowest value of CO₂ emissions is 23.25 gm/kWh at BMEP@2.38 bar for the chambered type

non-perforated muffler (Type-A). Similarly, at 1000 rpm the turbo perforated muffler (Type-D) shows maximum CO₂ emissions of 54.4 gm/kWh at BMEP@3.57 bar. The effect of perforation again has less effect in the case of the chamber type muffler for BMEP@3.57 bar, which are (1.01, 0.45, 3.72,1.24) gm/kWh for gasoline blends B₅, B₁₀ and B₁₅, respectively. Perforations lead to a maximum 59.3% increase in CO₂ emission in case of using the chamber type muffler with B₁₀ at BMEP@2.38 bar. Furthermore, the turbo type muffler gives a maximum 29.9% increase in CO₂ emission B₁₅ for BMEP@2.38 bar.

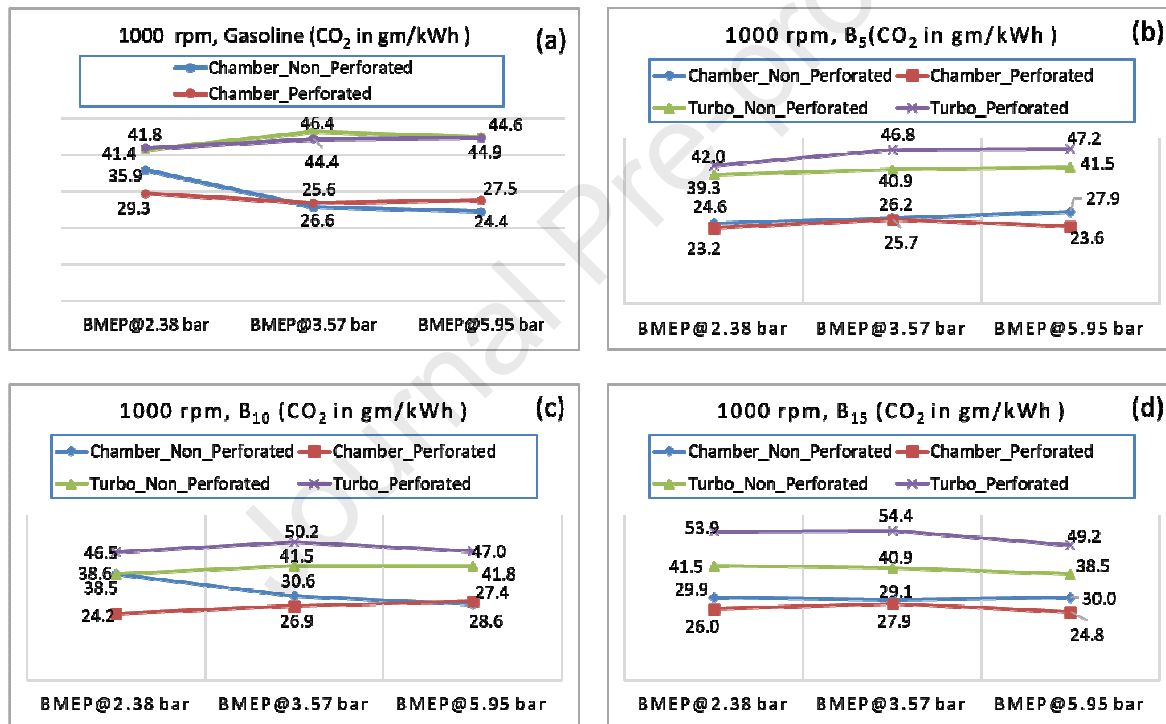


Fig.7 CO₂ response to engine BMEP, (a) Gasoline at 1000 rpm, (b) B₅ at 1000 rpm, (c) B₁₀ at 1000 rpm and (d) B₁₅ at 1000 rpm

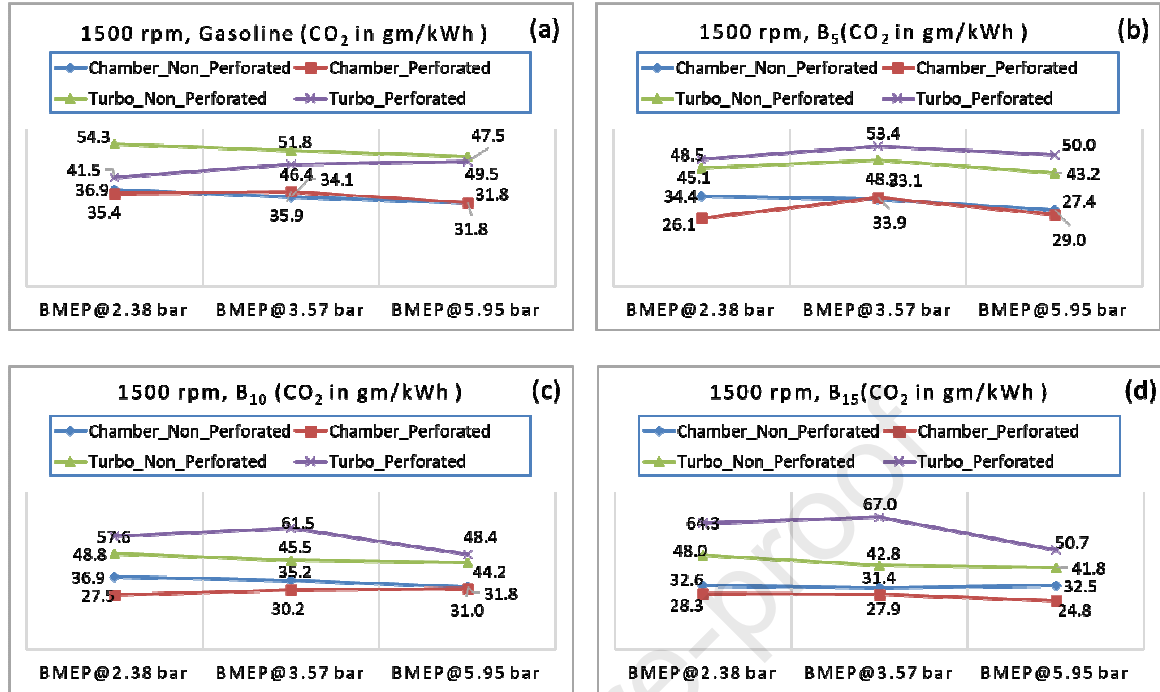


Fig.8 CO₂ response to engine BMEP, (a) Gasoline at 1500 rpm, (b) B₅ at 1500 rpm, (c) B₁₀ at 1500 rpm and (d) B₁₅ at 1500 rpm

Fig. 8 (a-d) show CO₂ response to engine BMEP at 1500 rpm for Gasoline, B₅, B₁₀ and B₁₅ respectively. The lowest CO₂ emissions at this speed are observed to be 24.15 gm/kWh. for the type-A muffler at 2 Nm. The highest CO₂ formation (67.04 gm/kWh) occurs at BMEP@3.57 bar for the type-D muffler. For the turbo type muffler, the effect of perforation enhances the CO₂ emissions by 56.7 % at BMEP@3.57 bar for B₁₅, while for the chamber type muffler, the effect of perforation enhances CO₂ emissions by 34.01% for B₁₀ at BMEP@2.38 bar. At BMEP@3.57 bar, for the Chamber type muffler, perforation has a negligible effect on CO₂ emissions (1.805, 0.79,4.96,3.5) gm/kWh. for all fuels (Gasoline, B₅, B₁₀ and B₁₅). The effect of perforations in the turbo type muffler has the highest impact on CO₂ emission with (5.41,5.19,16.02,24.26) gm/kWh for (Gasoline, B₅, B₁₀ and B₁₅)

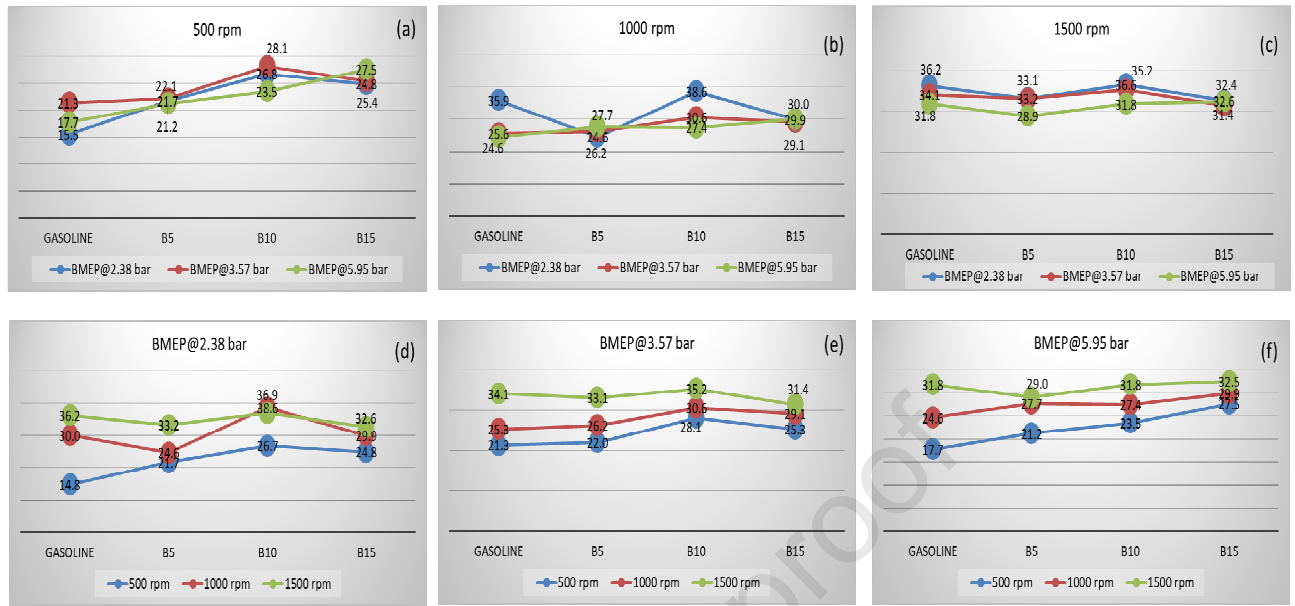


Fig.9 CO₂ response to fuel type at: (a) at 500 rpm, (b) 100 rpm, (c) 1500 rpm, (d) BMEP@2.38 bar, (e) BMEP@3.57 bar and (f) BMEP@5.95 bar

Figs. 9(a-f) show the CO₂ response to fuel change (Gasoline, B₅, B₁₀ and B₁₅). When gasoline is replaced with B₅, the emission levels are found to increase (0.79, 2.03, 1.35, -5.98, 0.90, 3.04) gm/kWh at (500 rpm, 1000 rpm, 1500 rpm, BMEP@2.38 bar, BMEP@3.57 bar and BMEP@5.95 bar). Similarly, when gasoline is replaced by blend B₁₀, the emission levels are also found to increase (6.77, 4.96, 3.38, 8.57, 5.30, 2.82) gm/kWh at (500 rpm, 1000 rpm, 1500 rpm, BMEP@2.38 bar, BMEP@3.57 bar and BMEP@5.95 bar). Furthermore, when gasoline is replaced by blend B₁₅, the emission levels are found to increase (gm/kWh) by % vol. at (500 rpm, 1000 rpm, 1500 rpm, BMEP@2.38 bar, BMEP@3.57 bar and BMEP@5.95 bar).

3.2 Muffler CFD Simulation results and discussions

To investigate the muffler exhaust performance, computational fluid dynamics simulation in ANSYS fluid was carried out. Solid model for the four mufflers were prepared, conforming to the geometries of fabricated ones. (Mishra et al. 2018) explained the step-by-step build-up

procedure for solid modelling using CATIA. Later, such models were imported to ANSYS fluid, the first step in ANSYS is to create 'mesh' model of the mufflers. Details of the mesh such as number of elements, number of nodes, element size, element type, etc. are automatically selected by ANSYS workbench. Here the element type auto-selected were tetrahedral with 18° curvature normal angle. Computational fluid dynamics (CFD) was pre-processed, which included defining the inlet and outlet surface of the control volume of a muffler.

The flow in the muffler was turbulent based on Reynolds number condition (Mishra et al.,2016 and Liu et al.,2020). The enclosing walls of all muffler were considered stationery with respect to the flowing exhaust gas with no slip boundary condition. With gross turbulent exhaust gas flow, the central plane contains streamline of flow as given in the fig. 3(a-b). The thermal boundary conditions were applied with suitable coefficient of thermal expansion (Mishra et al., 2016). And free stream temperature was considered to be of 300K with no diffusive flux. The commercial CFD software ANSYS-FLUENT in current case, used a pressure-based solver and adopted the SIMPLEC (Semi-Implicit Method for Pressure-Linked Equations-Consistent) pressure-velocity coupling algorithm (Mishra et al.,2016 and Liu et al.,2020) to generate the CFD outputs. Based on the emission gas composition and mass flow rate of constituent elements (CO, CO₂, HC, O₂), velocity stream line, density and enthalpies at the inlet are calculated. The executed program gave such output parameter for the entire fluid body present inside the muffler in between the inlet (Exhaust-manifold of the engine) and the outlet (tail-end of the muffler)

Table 4 shows the parameter required under inlet boundary conditions, which includes densities, enthalpies and viscosities for gasoline, B₅, B₁₀ and B₁₅. Table 5 shows the velocity (m/s) variation at inlet for all muffler design at gasoline, B₅, B₁₀ and B₁₅ use. For the type-A, type-B, type-C and type-D muffler. Table 6 shows other input parameters, such as temperature, mass

flow rate and heat transfer coefficient at the inlet of the muffler connected to the engine exhaust manifold. Table 7 shows the other input parameter and the mass fraction at inlet respectively as drawn from the emission measurement. The mesh model along with input parameters are loaded in the solver for output data generation.

Table 4 Parameters under inlet boundary conditions.

<i>Models/Parameters</i>	<i>Inlet Boundary</i>			
	Pure	B5	B10	B15
Density (gm/cm ³)	1.021	1.0271	1.0170	1.024
Enthalpy (kJ/kg)	163.68	156.90	161	159.2
Viscosity (kg/m-s)	0.00172	0.00172	0.00172	0.00172

Table 5 Velocity (m/s) variation at the inlet.

<i>Models/Blends</i>	<i>Pure</i>	<i>B5</i>	<i>B10</i>	<i>B15</i>
Type-A	0.1051	0.1084	0.1144	0.119
Type-B	0.1051	0.1084	0.1144	0.119
Type-C	0.1050	0.1085	0.1144	0.119
Type-D	0.1050	0.1085	0.1144	0.119

Table 6 Other input parameters

<i>Parameter</i>	<i>Pure</i>	<i>B5</i>	<i>B10</i>	<i>B15</i>
Temperature(⁰ C)	363	357	360	359
Mass Flow Rate (kg/sec) (10 ⁻⁵)	52	55	57	60
HT Coefficient (W/m ² K)	35	42	46	52

Table 7 Mass fraction at inlet (As input parameter)

<i>Cases/Gases</i>	<i>CO</i>	<i>NO_x</i>	<i>HC</i>	<i>CO₂</i>	<i>O₂</i>
Pure Gasoline	275.44×10^{-4}	1.1×10^{-4}	0.64×10^{-4}	624.1×10^{-4}	1766×10^{-4}
B ₅	33.1×10^{-4}	1.92×10^{-4}	0.82×10^{-4}	626×10^{-4}	1753×10^{-4}
B ₁₀	273×10^{-4}	1.42×10^{-4}	0.61×10^{-4}	605.7×10^{-4}	1797×10^{-4}
B ₁₅	267.7×10^{-4}	2.12×10^{-4}	0.556×10^{-4}	771.2×10^{-4}	1640×10^{-4}

The pressure-based solver discussed was used in this study, where heat transfer is addressed through the energy model and assumed that the flow of heat occurs from the hot exhaust gas to the walls of the muffler. As the exhaust gas moves faster, geometrical obstruction opposes the flow and creates backpressure. The mesh convergence and grid-independent tests were carried out through mesh quality check functionality to ensure correction in grid formation and that of mesh size. The figures (10-13) show muffler performance parameters for all four models. Fig. 10 shows the velocity streamlines from inlet to outlet, the maximum velocity of 0.28 m/s occurs at the type-B muffler, while the lowest 0.1643 m/s observed in the case of type-D muffler. The emission particulate concentration was observed at the inlet pipe due to the gas flow, in case of type-A muffler, while such concentration is found in the baffle plate region. Similarly, in type-C muffler, such segregation occurs in outer pipes within muffler chamber. While in case of type-D muffler, the emission particulate sprinkled through out the chamber. Perforation in both B and D case is created intentionally created to improve circulation and to observe if such circulation has effect on temperature, back pressure, density of emission constituents. As, it is observed, any change in muffler surface temperature, affects NO_x formation (Mishra et al.,2016).

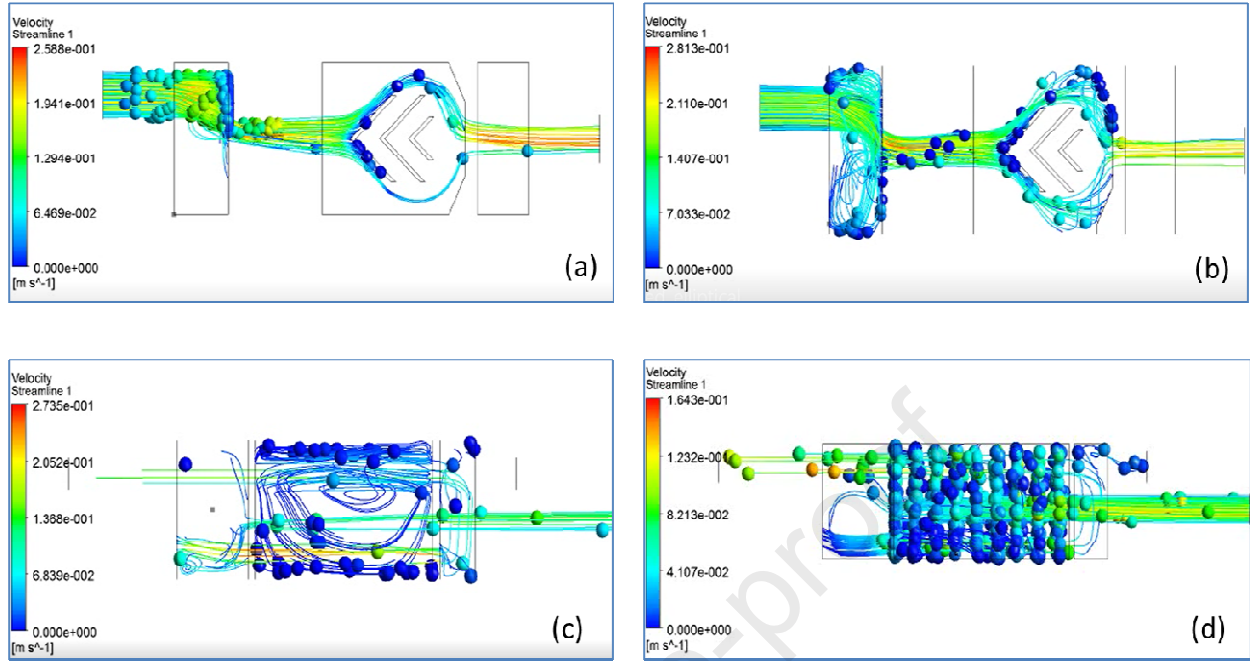


Fig.10 Velocity streamline from CFD simulation of: a: Type-A muffler, b: Type-B muffler, c: Type-C muffler and d: Type-D muffler

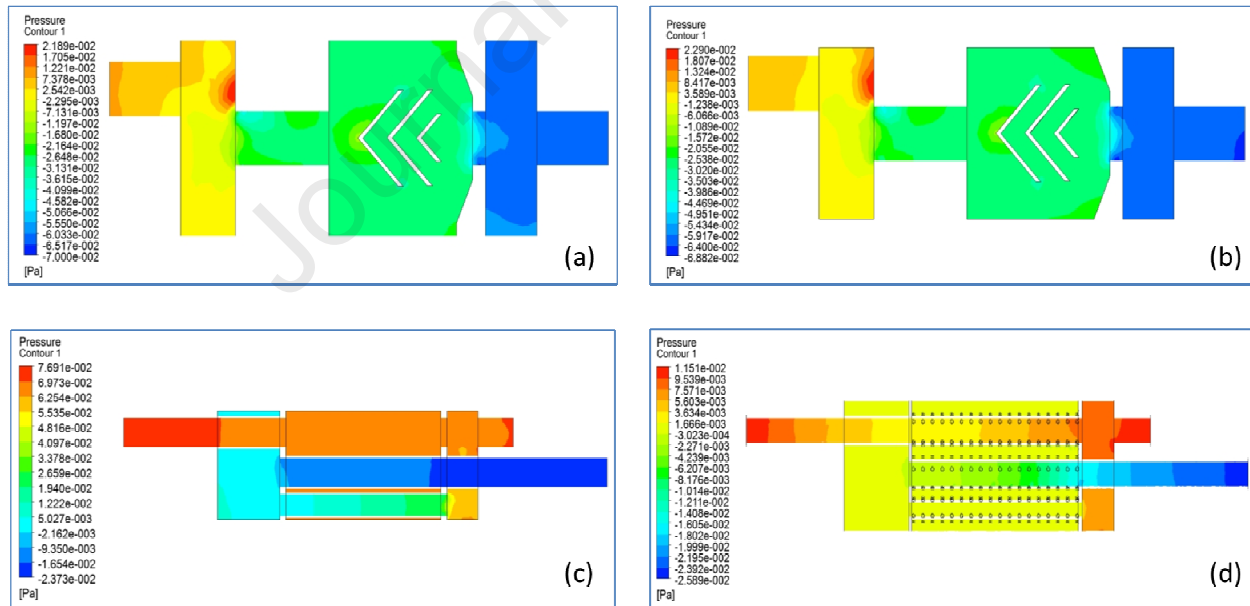


Fig.11 Backpressure from CFD simulation of: a: Type-A muffler, b: Type-B muffler, c: Type-C muffler and d: Type-D muffler

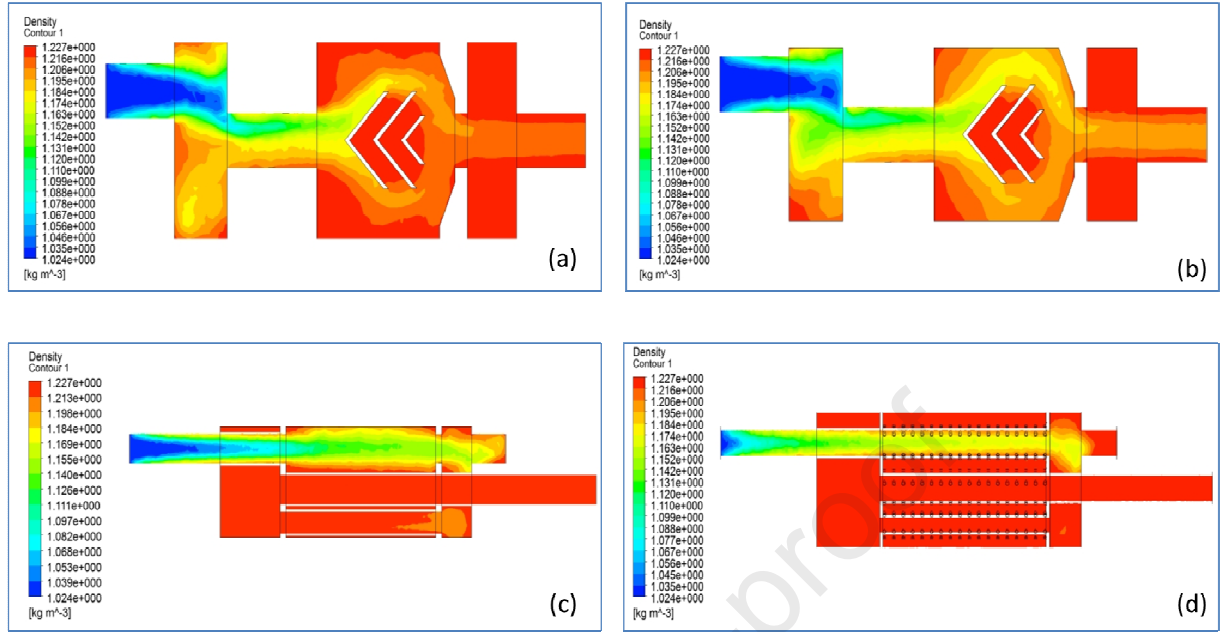


Fig.12 Emission gas density CFD simulation of: a: Type-A muffler, b: Type-B muffler, c: Type-C muffler and d: Type-D muffler

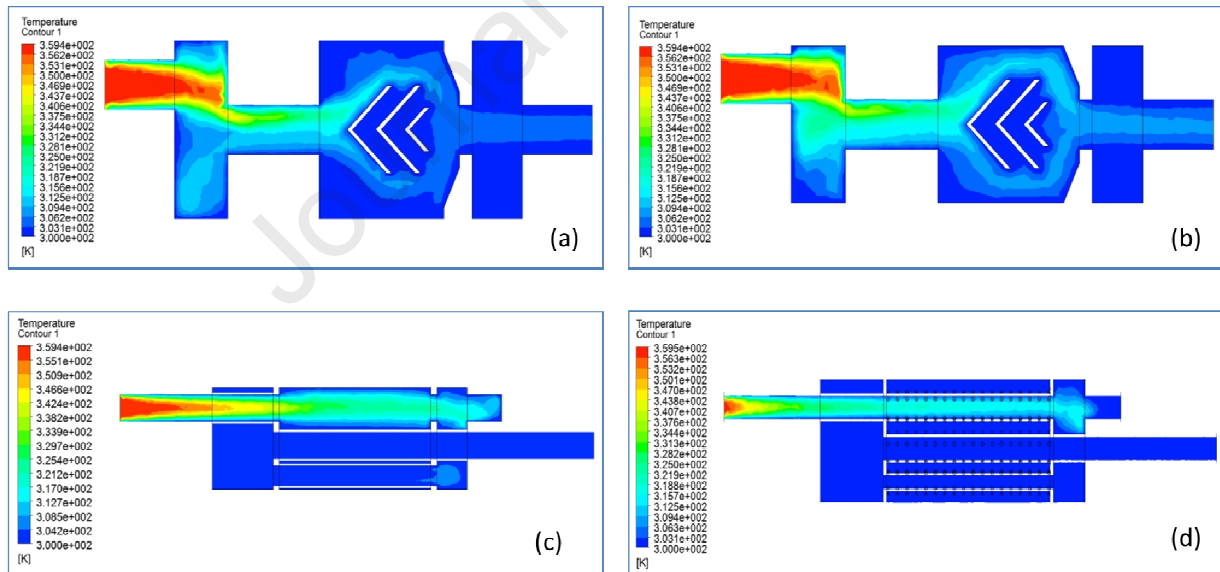


Fig.13 Emission gas temperature from CFD simulation of: a: Type-A muffler, b: Type-B muffler, c: Type-C muffler and d: Type-D muffler

Fig. 11 shows the back-pressure mapping of the four different mufflers, the results were obtained from CFD simulation. The change in back pressure, significantly affect the noise and attenuation in the muffler. Monitoring of such parameter, helps understanding the gas behavior and its relation to noise, frequency and wavelength etc. The highest back pressure of 0.0769 Pa was observed for turbo non-perforated muffler, while the lowest of 0.0151 Pa found in the case of turbo-perforated one. Such pressure is higher in the inlet zone, while it decreases towards outlet. Perforation, enhances back pressure in case of chamber type muffler, while it diminishes in case of turbo muffler.

Fig. 12 shows the density distribution in the muffler control volume. Not much significant variation in density is observed. The density of the exhaust gas is more in the vicinity of the baffle plate in the case of chamber type muffler, while for turbo pipe type muffler it is more in the pipe adjacent to the inlet. The reason for this is the obstruction offered by the baffle plate and the feedback loop in respective cases. Such density variation has inverse square root relation with the sound velocity and frequency. Multiple muffler designs show, optimized geometry for acceptable noise characteristics.

Fig. 13 shows the temperature distribution of the four different models. The distribution of temperature is more in the turbo mufflers compared to chambered type mufflers. In table 8 the key exhaust performance parameters are summarized. The highest temperature observed in the case of the inlet zone and the obstructed part of the muffler as described earlier. It is because of the retention of hot gas for more time in the vicinity of the portions discussed.

Table 8 Summary of key exhaust performance parameters.

Muffler detail and blend detail	Maximum value of velocity in (m/s)	Maximum value of density in (kg/m ³)	Maximum value of backpressure in (Pa)x10 ⁻²	Maximum value of exhaust temperature in (°K)
Type-A&B muffler using pure gasoline	0.24	1.22	6.2	362
Type-C&D muffler using pure gasoline	0.146	1.25	1.4	362
Type-A&B muffler using B5	0.25	1.22	6.7	357
Type-C&D muffler using B5	0.152	1.27	1.49	357
Type-A&B muffler using B10	0.25	1.22	7.3	360
Type-C&D muffler using B10	0.158	1.26	1.5	360
Type-A&B muffler using B15	0.27	1.22	7.7	359
Type-C&D muffler using B15	0.164	1.30	1.65	359

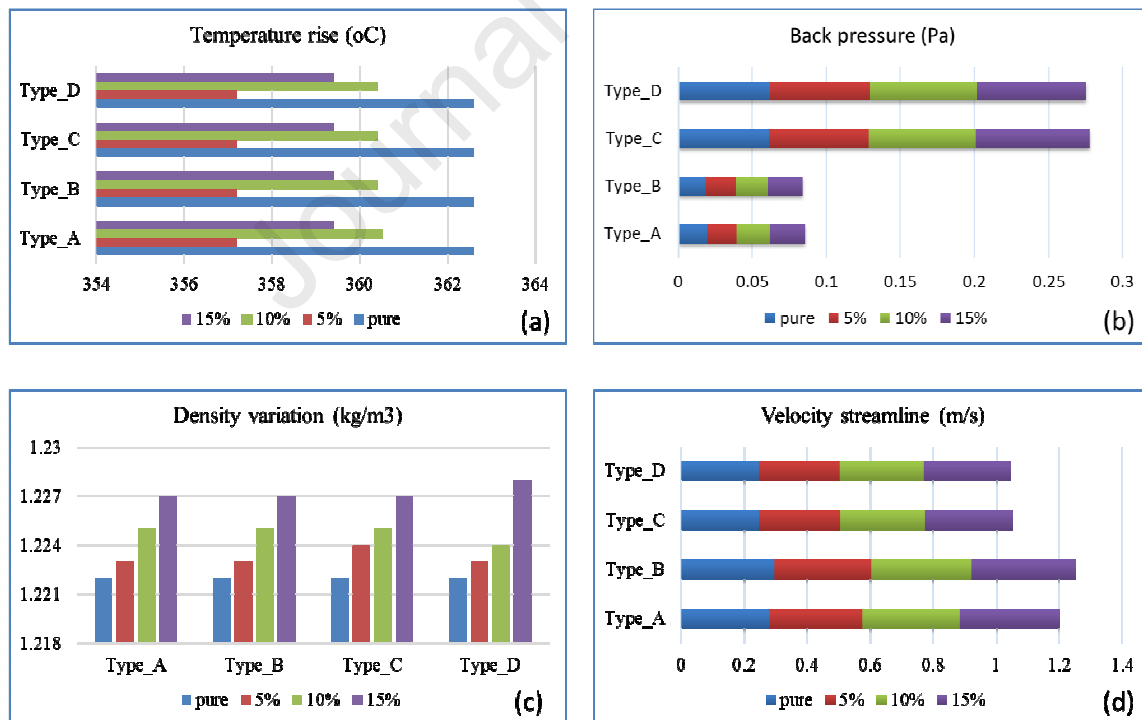


Fig.14 Bar chart of muffler performance, (a) Temperature rise, (b) back pressure variations, (c) density variation and (d) velocity stream line

Fig.14(a-d) show the performance of the mufflers, which include surface temperature, back pressure, density and streamline velocity respectively plotted through bar chart comparison. The surface temperature (fig.14-a) is almost independent to the muffler design. This is highest in case of pure gasoline fuel and lowest in the case of blend B₁₀. It may be due to complete combustion of fuel compared to pure gasoline, B₅ and B₁₅. The backpressure (fig. 14-b) is the higher in the case of the chambered type (Type-A and Type-B) mufflers as compared to the turbo types (Type-C and Type-D). Fig. 9-c shows the density variation of exhaust gas, which increases with % increase of methanol in the blend. As we proceed to the higher order of the blend, the combustion improves and yields dense emission constituents. As shown in fig. 14-d, the velocity streamline is higher, in the case of the chamber type design, as the path is simple, while in the case of the turbo design the path is circulatory and more complex.

5. Fuel replacement response to Noise and performance

The fuel replacement to gasoline-methanol blend has observable effect on noise and performance. During lower rpm, the brake power response to rpm is plotted in fig. 15-a, shows higher blend mixture has elevated brake power compared to pure gasoline and lower blends.

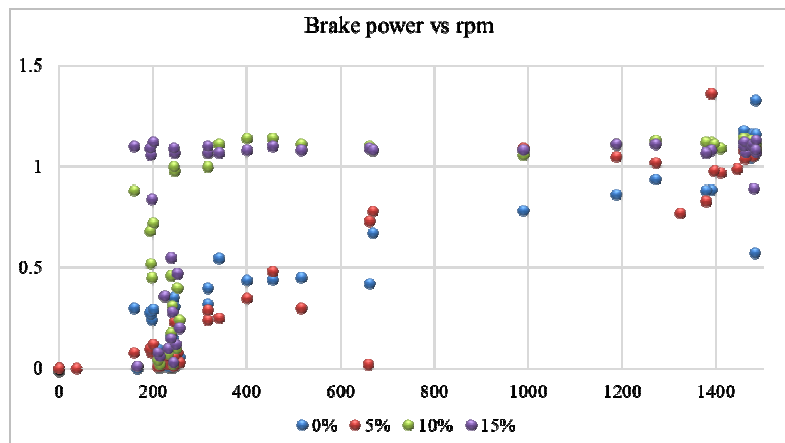


Fig.15 (a) Brake power response to rpm for different fuel replacement

But in the higher speed, the difference decreases and at 1500 rpm, there is 50% more brake power achieved due to 15% blend. Fig. 15-b shows the noise level recorded at different speeds. Blend fuels show lower noise level than gasoline, except at 600 rpm, where B₅ has highest noise. But at 800 rpm or further always with higher % of methanol, diminish the noise level from engine

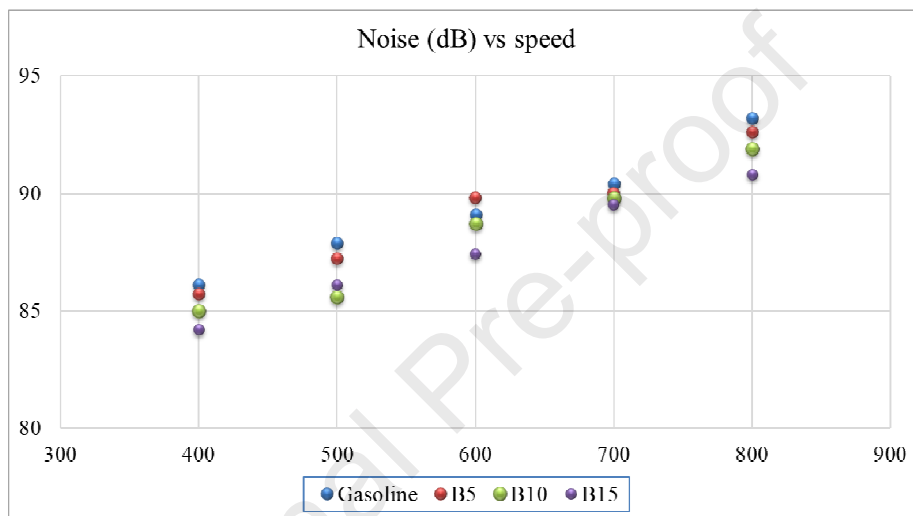


Fig.15 (b) Noise response to rpm for different fuel replacement

6. Sustainability of Muffler modification and fuel replacement

The sustainability of multiple muffler design exchange and fuel replacement is worth discussing here. The maximum blending considered here is up to 15%. A higher amount of methanol content we have not encouraged in this analysis, reason is the toxicity of methanol content and also the flameless combustion. Second feasibility; methanol is easily available and it can be produced in the Petro-chemical facilities with minimal additional investment. There is no change in engine infrastructure required for such small fuel exchanges. The direct advantage is that the CO₂ formation is reduced as compared to pure gasoline. This direct benefit is available for no

changes in engine structure or materials and minimal costs in fuel preparation as no separate blending facility is needed. Therefore, the improved impact on the environment from the reduction of engine emissions of CO₂ outweighs the potential cost of blending and providing this fuel directly to the pump for vehicle users. Furthermore, it can potentially reduce the demand for pure gasoline by 15% volume. This could result in financial benefits for oil companies. It has the potential of creating a new 'Methanol Economy' which can create opportunities for economic prosperity.

6. Conclusion

This study has investigated how it is possible to improve the CO₂ emissions from a gasoline engine by using blended gasoline-methanol fuels without negatively impacting the engine performance, or having a hugely detrimental effect on the engine structure. Only a small modification external to the engine is exhibited.

In addition to the gasoline-methanol blends, the design of the muffler has also been investigated for its effect on CO₂ emissions. The key findings are summarized as:

- Chambered type non-perforated muffler (Type-A) is best among all designs for reduced CO₂ emissions.
- Turbo perforated (Type-D) muffler has the most CO₂ emissions compared to all designs.
- For chambered type muffler, the effect of perforation is negligible at BMEP@3.57 bar for all range of engine speed (500, 1000,1500) rpm.
- The effect of perforation on CO₂ emission is maximum at BMEP@3.57 bar for turbo type muffler.

- At constant speed, the CO₂ emissions are higher for lower BMEP and at constant BMEP, CO₂ emissions are lower for lower speeds.

Such minor modifications have immediate implication to the automotive sectors and fuel manufacturers. The introduction of methanol could reduce the burden on petroleum reserves with the benefits of reduced CO₂ emissions. The limitation of the current analysis is that the methanol is restricted to 15% in the blend. This is to eliminate the toxic effect and rapid degradation of engine components. Testing different capacity engines with a higher percentage of methanol (25%, 30% and 50%) is the future extension of this research work. Also, further study on combined effect of muffler design change and emission formation on noise control efficiency is highly encouraging.

7. Acknowledgement

I am very much thankful to the All India Council for Technical Education and Training (AICTE), New Delhi for funding this research. The funding of AICTE through RPS grant-in-aid to carry out our research project entitled “Advanced Engine Technology for Sustainable Development of Automotive Industry” with grant number ‘20/AICTE/RIFD/RPS (POLICY-III) 43/2012-13’ is here acknowledged. We are thankful to the computational facilities at KIIT University, School of Mechanical Engineering to carry out the simulation work of this research. We are also thankful to our undergraduate students, Harshit Kumar Mishra, Sourav Kumar Kar and postgraduate student Abhishek Kashyap for their dedicated work in this project and their hard work on simulation and testing is here acknowledged. The collaboration with the School of Engineering and Sustainable Development, De Montfort University, Leicester and School of Engineering, Technology and Design, Canterbury Christ Church University, Canterbury in the United Kingdom is here acknowledged.

Reference

- Athanasopoulou, L., Bikas, H., & Stavropoulos, P. (2018). *Comparative Well-to-Wheel Emissions Assessment of Internal Combustion Engine and Battery Electric Vehicles. Procedia CIRP*, 78, 25–30. doi:10.1016/j.procir.2018.08.169
- Aye, G. C., & Edoja, P. E., 2017. *Effect of economic growth on CO₂ emission in developing countries: Evidence from a dynamic panel threshold model*. *Cogent Economics & Finance*, 5(1). doi:10.1080/23322039.2017.1379239.
- Beatrice, C., Di Blasio, G., & Belgiorno, G. (2017). Experimental analysis of functional requirements to exceed the 100 kW/l in high-speed light-duty diesel engines. *Fuel*, 207, 591–601. doi:10.1016/j.fuel.2017.06.112
- Belgiorno, G., Boscolo, A., Dileo, G., Numidi, F. et al., "Experimental Study of Additive-Manufacturing-Enabled Innovative Diesel Combustion Bowl Features for Achieving Ultra-Low Emissions and High Efficiency," SAE Technical Paper 2020-37-0003, 2020, <https://doi.org/10.4271/2020-37-0003>.
- Çelik, M., & Bayindirli, C. (2020). *Enhancement performance and exhaust emissions of rapeseed methyl ester by using n-hexadecane and n-hexane fuel additives. Energy*, 117643. doi:10.1016/j.energy.2020.117643
- Di Blasio, G., Beatrice, C., Belgiorno, G., Pesce, F. C., & Vassallo, A. (2017). Functional Requirements to Exceed the 100 kW/l Milestone for High Power Density Automotive Diesel Engines. *SAE International Journal of Engines*, 10(5). <http://doi:10.4271/2017-24-0072>.
- Di Blasio, G., Beatrice, C., Ianniello, R., Pesce, F. et al., "Balancing Hydraulic Flow and Fuel Injection Parameters for Low-Emission and High-Efficiency Automotive Diesel Engines," *SAE Int. J. Adv. & Curr. Prac. in Mobility* 2(2):638-652, 2020, <https://doi.org/10.4271/2019-24-0111>.
- Driving the Future Today A strategy for ultra-low emission vehicles in the UK, Office for low emission vehicle, Sept-2013, www.gov.uk/loev
- Ekwurzel, B., Boneham, J., Dalton, M.W. et al., 2017. The rise in global atmospheric CO₂, surface temperature, and sea level from emissions traced to major carbon producers. *Climatic Change* **144**, 579–590. <https://doi.org/10.1007/s10584-017-1978-0>
- E Terrenoire et al. 2019 *Environ. Res. Lett.* 14 084019.
- Gambill, W.R., 1959, "How to estimate mixtures viscosities", *Chemical Engineering*, 66, pp. 151-152.

- Gupta, A., Mishra, P.C., 2019. *Optimization of emission characteristics of spark ignition engine with chambered straight muffler running in methanol blend: An engine development technique for environmental sustainability*. *Journal of Cleaner Production*, 238. <https://doi.org/10.1016/j.jclepro.2019.117778>
- Hashimoto, R. Mori, G., Yasir, M., Tröger, U., Wieser, H. Condensate in the muffler of automotive exhaust system NACE - International Corrosion Conference Series 2013, 10p Corrosion 2013; Orlando, FL; United States; 17 March 2013 through 21 March 2013; Code 98665.
- Inoue, Y., Kikuchi, M. Present and future trends of stainless steel for automotive exhaust system Nippon Steel Technical Report Issue 88, July 2003, Pages 62-69.
- Kianfar, E., Salimi, M., Pirouzfard, V., & Koohestani, B., 2017. *Synthesis of modified catalyst and stabilization of CuO/NH₄-ZSM-5 for conversion of methanol to gasoline*. *International Journal of Applied Ceramic Technology*, 15(3), 734–41. doi:10.1111/ijac.12830
- L. Y. Liu, X. Zheng, Z. Y. Hao, and Y. Qiu. A computational fluid dynamics approach for full characterization of muffler without and with exhaust flow. (2020). *Physics of Fluids*, 32(6), 066101. <http://doi:10.1063/5.0008340>.
- Maples, R.E., 2000, "Petroleum Refinery Process Economics", PennWell, ISBN 978-0-87814-779-3.
- Mishra, P.C., Gupta, A., Kumar, A., & Bose, A., 2020. *Methanol and petrol blended alternate fuel for future sustainable Engine: A performance and emission analysis*. *Measurement*, 107519. <http://doi:10.1016/j.measurement.2020.107519>
- Mourad, M., & Mahmoud, K., 2019. *Investigation into SI Engine Performance Characteristics and Emissions fuelled with Ethanol/Butanol-Gasoline Blends*. *Renewable*.
- NPTL course from IIT Kanpur: <https://nptel.ac.in/courses/112/104/112104033/>
- Olabi, A. G., Maizak, D., & Wilberforce, T., 2020. Review of the regulations and techniques to eliminate toxic emissions from diesel engine cars. *Science of The Total Environment*, 141249. <http://doi:10.1016/j.scitotenv.2020.141249>
- Piotr Lijewski, et al., *Transportation Research Part D*, <https://doi.org/10.1016/j.trd.2019.11.012>
- Ramasso, E., Butaud, P., Jeannin, T., Sarasini, F., Placet, V., Godin, N., ... Gabrion, X. (2020). *Learning the representation of raw acoustic emission signals by direct generative modelling and its use in chronology-based clusters identification*. *Engineering Applications of Artificial Intelligence*, 90, 103478. doi:10.1016/j.engappai.2020.103478

- Reddy, AK (2017). A Critical Review on Acoustic Methods & Materials of a Muffler. *Materials Today: Proceedings*, 4(8), 7313–7334. doi:10.1016/j.matpr.2017.07.061
- Shrivastava, P., Salam, S., Verma, T. N., & Samuel, O. D., 2019. *Experimental and empirical analysis of an IC engine operating with ternary blends of diesel, karanja and roselle biodiesel*. *Fuel*, 116608. <http://doi:10.1016/j.fuel.2019.116608>.
- Udara Willhelm Abeydeera, L. H., Wadu Mesthrige, J., & Samarasinghalage, T. I. (2019). *Global Research on Carbon Emissions: A Scientometric Review*. *Sustainability*, 11(14), 3972. doi:10.3390/su11143972.
- Vassallo, A., Beatrice, C., Di Blasio, G., Belgiorno, G., Avolio, G., & Pesce, F. C. "The Key Role of Advanced, Flexible Fuel Injection Systems to Match the Future CO₂ Targets in an Ultra-Light Mid-Size Diesel Engine," SAE Technical Paper 2018-37-0005, 2018, <https://doi.org/10.4271/2018-37-0005>.
- Venkata Sundar Rao, K., Kurbet, S. N., & Kuppast, V. V. (2018). *A Review on Performance of the IC Engine Using Alternative Fuels*. *Materials Today: Proceedings*, 5(1), 1989–1996. doi:10.1016/j.matpr.2017.11.303.
- Verhelst, S., Turner, J. W., Sileghem, L., & Vancoillie, J. (2019). *Methanol as a fuel for internal combustion engines*. *Progress in Energy and Combustion Science*, 70, 43–88. doi:10.1016/j.peccs.2018.10.001.

Abbreviations

CO ₂ -	Carbon dioxide	PHEV-	Plug-in hybrid electric vehicle
CFD-	Computational fluid dynamics	BEV-	Battery electric vehicle
CO-	Carbon monoxide	kW/l -	Kilowatt per liter
NO _x -	Nitrogen Oxides	kWh -	Kilowatt hour
HC-	Hydrocarbon	HF -	Hydraulic flow
THC-	Total hydrocarbon	SI -	Spark ignition engine

EG-	Economic growth	VCN-	Variable blend number
ICE-	Internal combustion Engine	OCT -	Octane number
ANN-	Artificial neural network		
ASTM-	American standard of testing and method		
GI-	Galvanized iron sheet		
E-	Young's modulus		
v-	Poisson's ratio		
BMEP-	Brake mean effective pressure		
B5/B10/B15	Gasoline-Methanol blend		
BTE -	Brake thermal efficiency		
HRR -	Heat dissipation rate		

649

650

651

652

653

654

655

656

657

658

659

Table captions

Table 1 Comparative values of blend with respect to gasoline and methanol

Table 2: Specification of water-cooled Eddy current dynamometer with 38 kW power rating (Mishra et al., 2020)

Table 3: Specification of Horiba Mexa 584-L emission gas analyzer (Mishra et al., 2020)

Table 4: Parameters under inlet boundary conditions.

Table 5. Velocity (m/s) variation at the inlet.

Table 6: Other input parameters

Table 7: Mass fraction at inlet (As input parameter).

Table 8: Summary of key exhaust performance parameters

Figure captions

Fig. 1: World Carbon dioxide emission levels

Fig. 2: Muffler manufacturing, (a) Type A: Chamber non-perforated, (b) Type B: Chamber perforated, (c) Type C: Turbo non-perforated and (d) Type D: turbo perforated

Fig. 3: Exhaust gas path (Mishra et al., 2020) in: (a) Chamber type muffler, (b) Turbo type muffler

Fig. 4: Emission measurement, (a) Emission data acquisition, (b) performance data acquisition, (c) emission sensing at exhaust and (d) Engine test bed

Fig. 5: Dynamometer arm and emission analyzer in measuring mode

Fig. 6: CO₂ response to engine torque, (a) Gasoline at 500 rpm, (b) B₅ at 500 rpm, (c) B₁₀ at 500 rpm and (d) B₁₅ at 500 rpm

Fig. 7: CO₂ response to engine torque, (a) Gasoline at 1000 rpm, (b) B₅ at 1000 rpm, (c) B₁₀ at 1000 rpm and (d) B₁₅ at 1000 rpm

Fig. 8: CO₂ response to engine torque, (a) Gasoline at 1500 rpm, (b) B₅ at 1500 rpm, (c) B₁₀ at 1500 rpm and (d) B₁₅ at 1500 rpm

Fig. 9: CO₂ response to fuel type at: (a) at 500 rpm, (b) 100 rpm, (c) 1500 rpm, (d) 2 Nm, (e) 3 Nm and (f) 5 Nm

Fig. 10: Velocity stream line from CFD simulation of: (a) Type-A muffler, (b) Type-B muffler, (c) Type-C muffler and (d) Type-D muffler

Fig. 11: Back pressure from CFD simulation of: (a) Type-A muffler, (b) Type-B muffler, (c) Type-C muffler and (d) Type-D muffler

Fig.12: Emission gas density from CFD simulation of: (a) Type-A muffler, (b) Type-B muffler, (c) Type-C muffler and (d) Type-D muffler

Fig.13: Emission gas temperature from CFD simulation of: (a) Type-A muffler, (b) Type-B muffler, (c) Type-C muffler and (d) Type-D muffler

Fig.14: Bar chart of muffler performance, (a) Temperature rise, (b) back pressure variations, (c) density variation and (d) velocity stream line

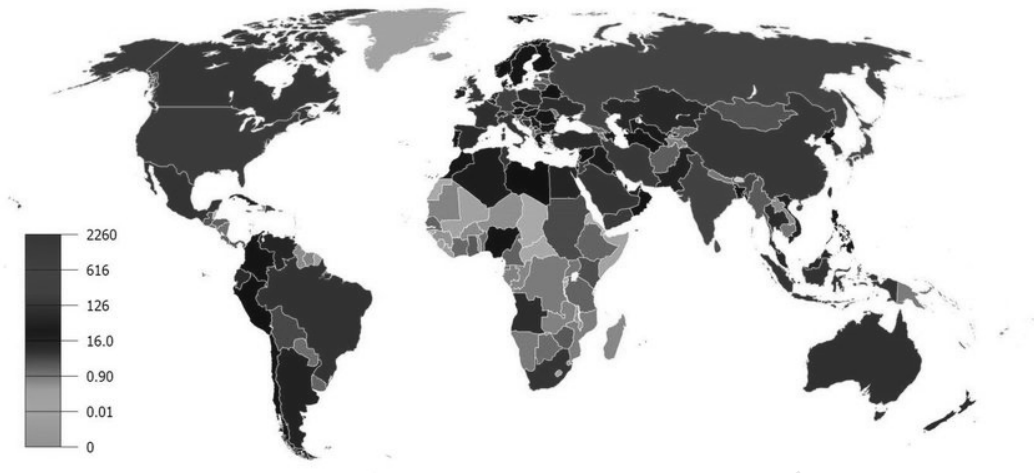
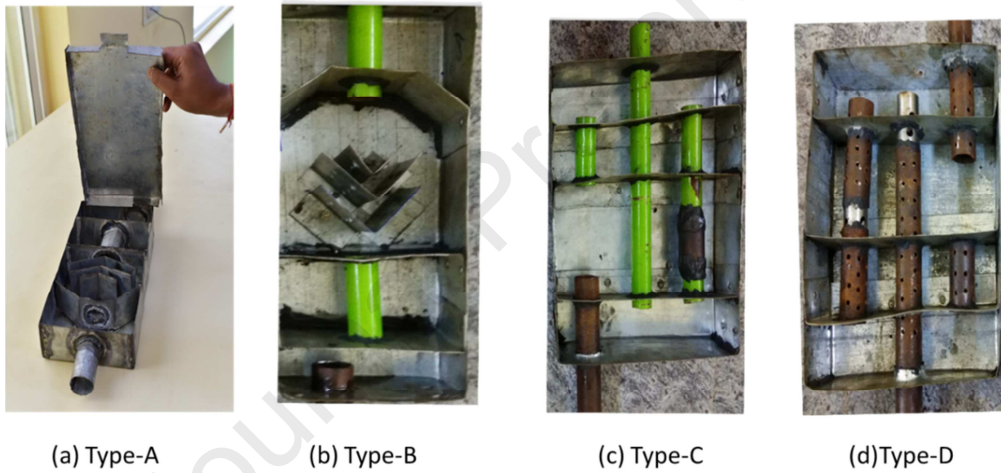


Fig.1 World Carbon dioxide emission levels (<http://lert.co.nz/map>)



(a) Type-A

(b) Type-B

(c) Type-C

(d) Type-D

Fig. 2 Muffler manufacturing, (a) Type A: Chamber non-perforated, (b) Type B: Chamber perforated, (c) Type C: Turbo non-perforated and (d) Type D: turbo perforated

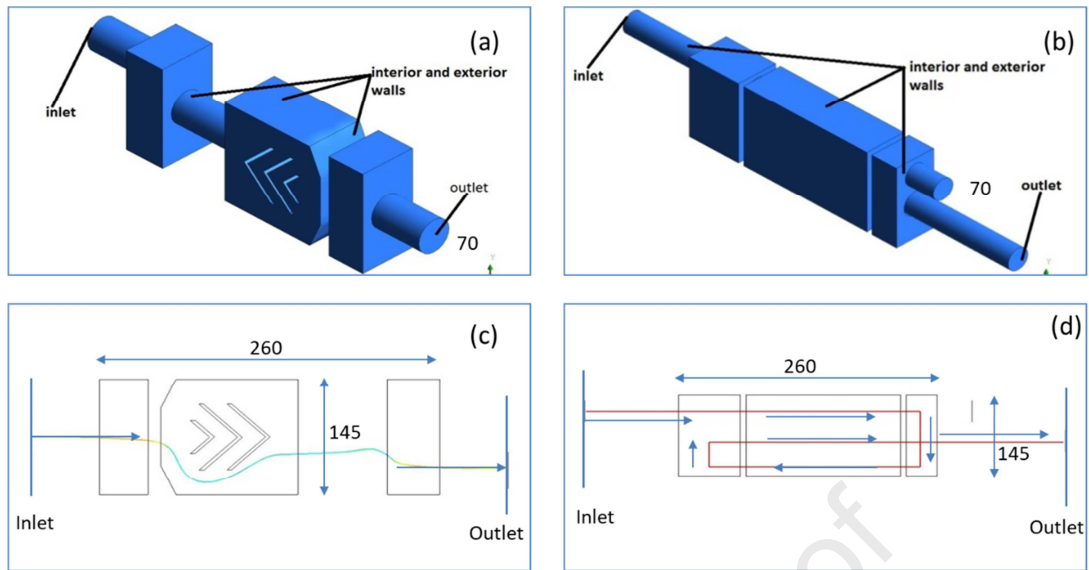


Fig.3 Exhaust gas path (Mishra et al., 2020) in, a: Chamber type muffler fluid content, b: Turbo type muffler fluid content, c: Evaluated fluid path-chambered type and d: Evaluated fluid path-turbo type

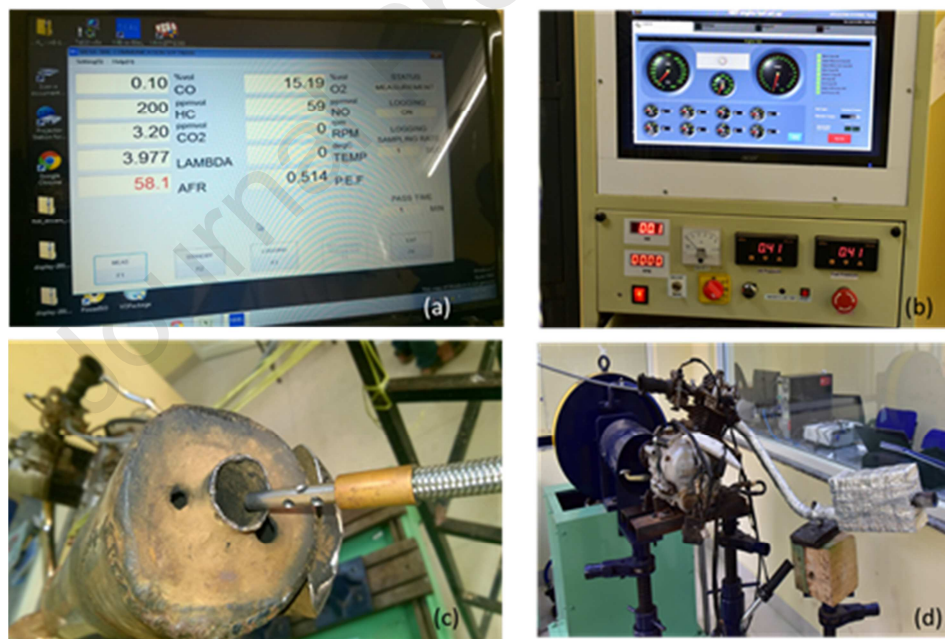


Fig.4 Emission measurement, a: Emission data acquisition, b: performance data acquisition, c: emission sensing at the exhaust and d: engine testbed

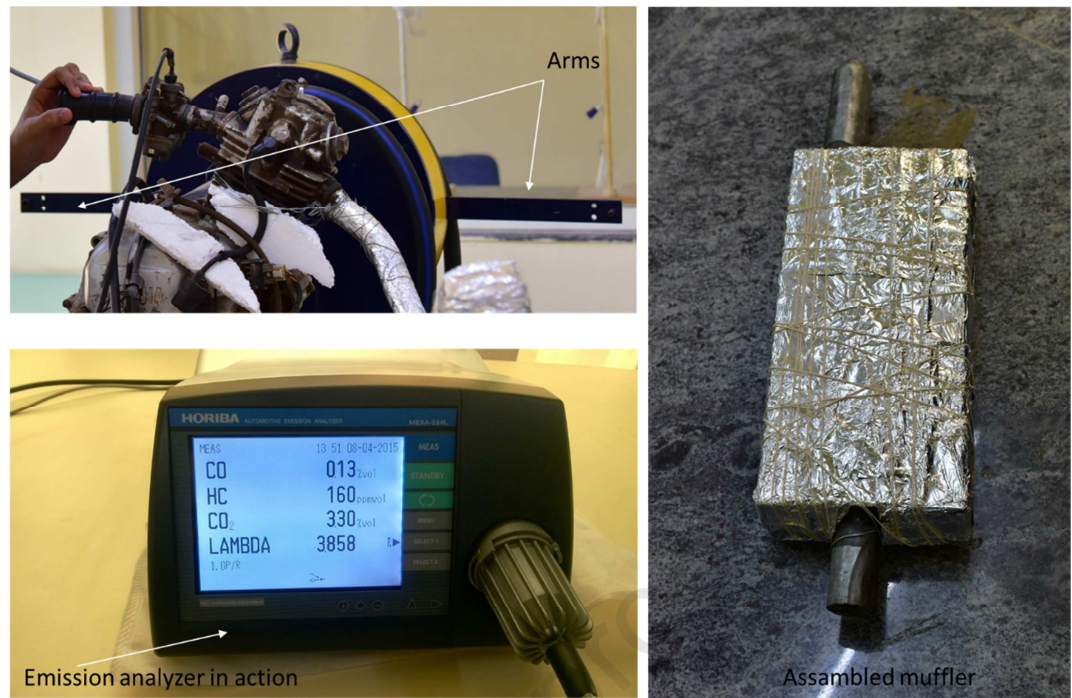


Fig. 5 Dynamometer arm, emission analyzer in measuring mode and assembled muffler

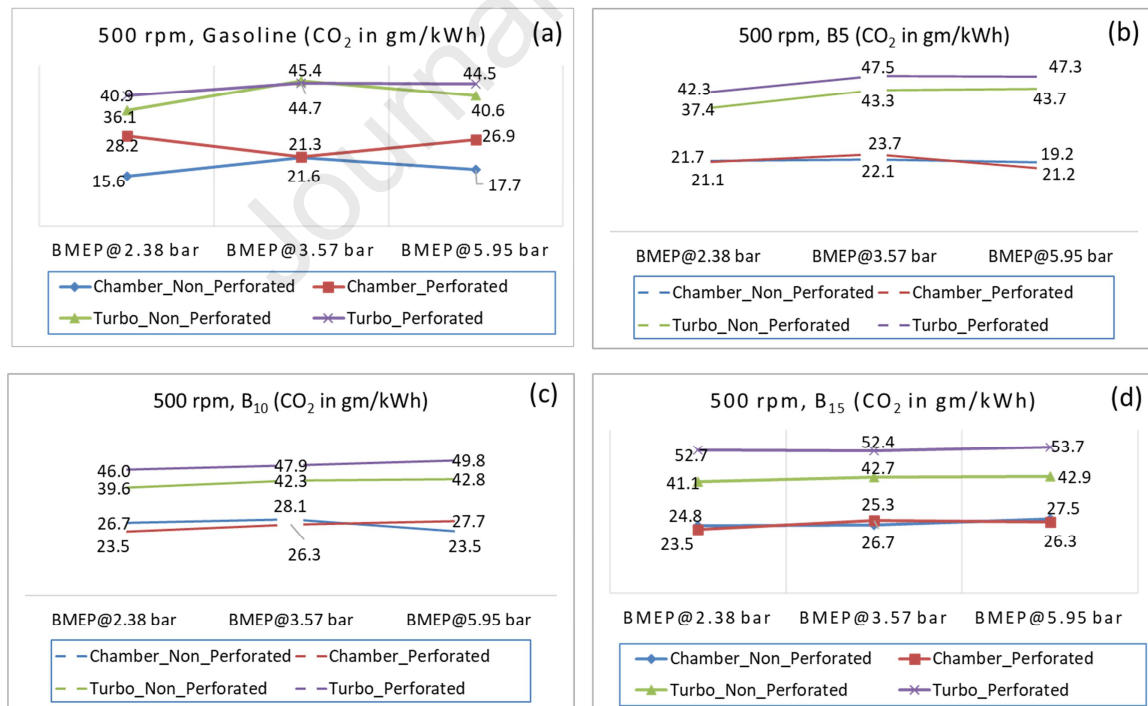


Fig.6 CO_2 response to engine BMEP, (a) Gasoline at 500 rpm, (b) B₅ at 500 rpm, (c) B₁₀ at 500 rpm and (d) B₁₅ at 500 rpm

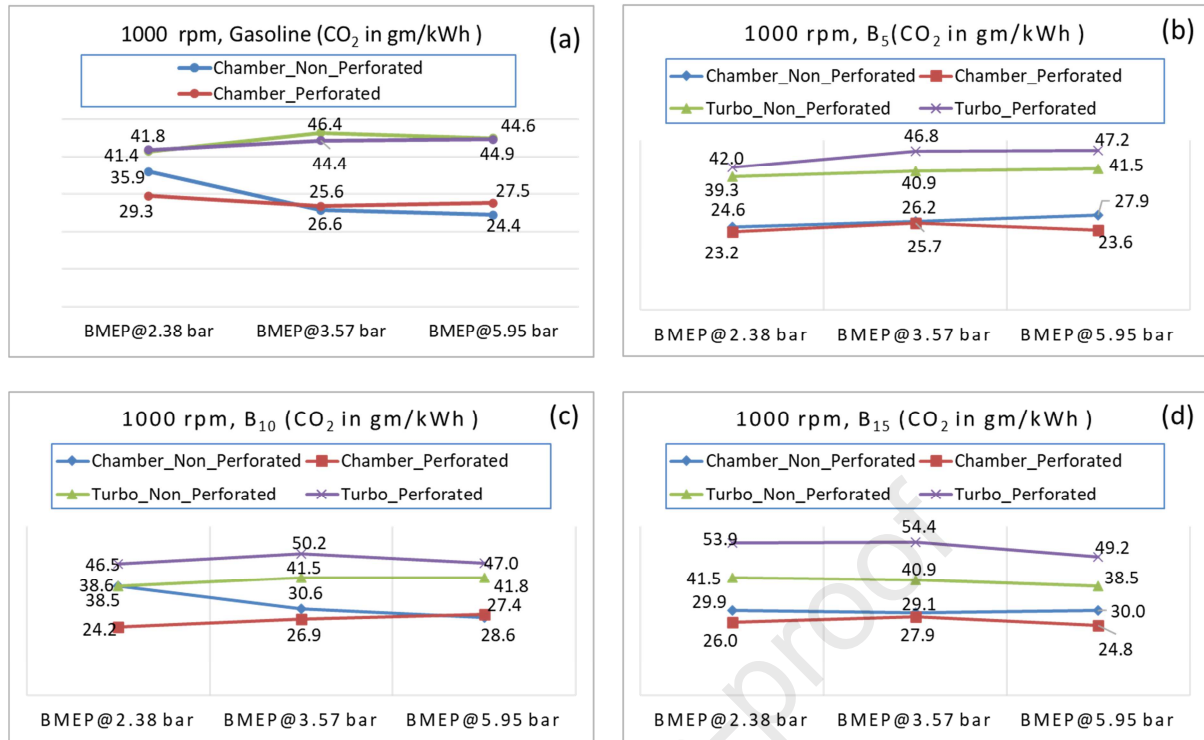


Fig.7 CO₂ response to engine BMEP, (a) Gasoline at 1000 rpm, (b) B₅ at 1000 rpm, (c) B₁₀ at 1000 rpm and (d) B₁₅ at 1000 rpm

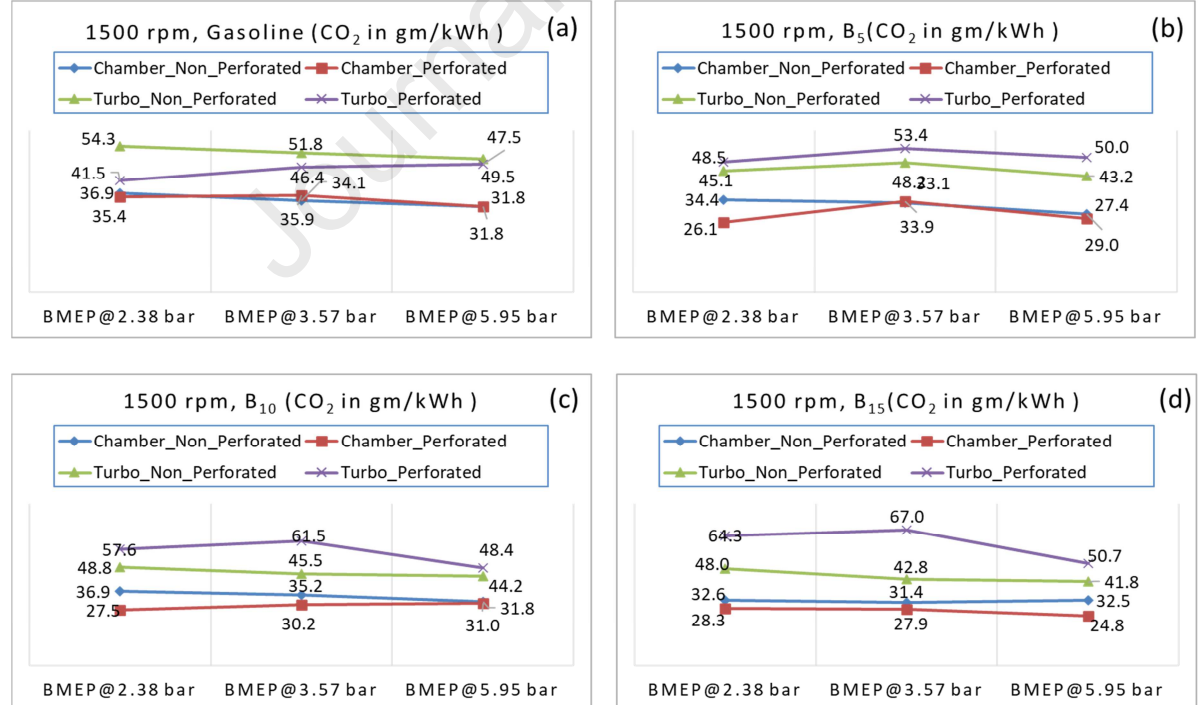


Fig.8 CO₂ response to engine BMEP, (a) Gasoline at 1500 rpm, (b) B₅ at 1500 rpm, (c) B₁₀ at 1500 rpm and (d) B₁₅ at 1500 rpm

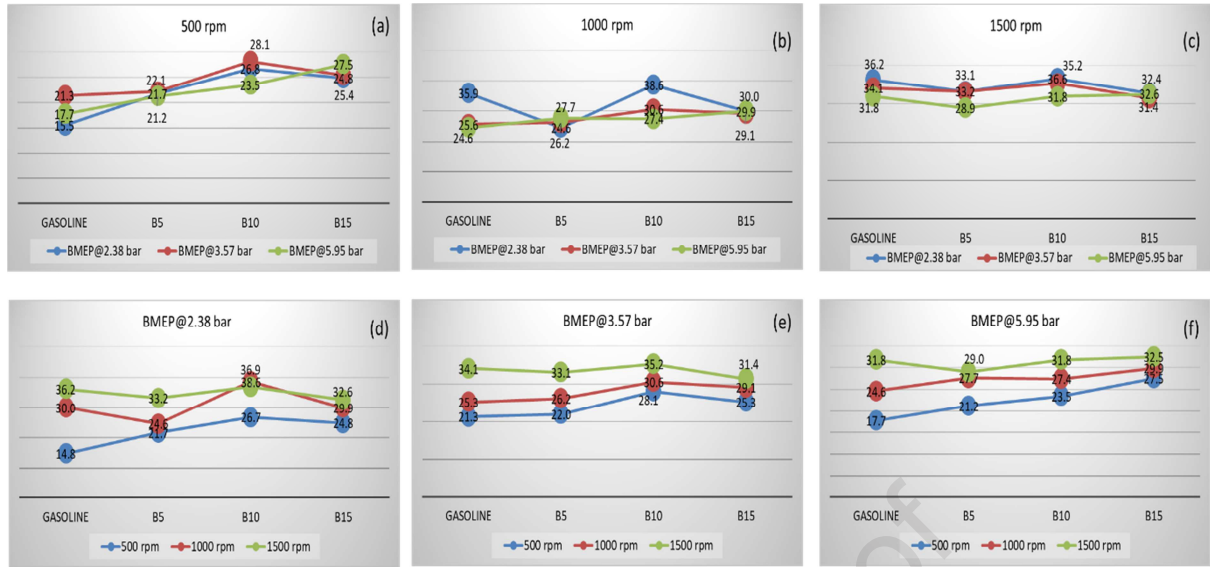


Fig.9 CO₂ response to fuel type at: (a) at 500 rpm, (b) 100 rpm, (c) 1500 rpm, (d) BMEP@2.38 bar, (e) BMEP@3.57 bar and (f) BMEP@5.95 bar

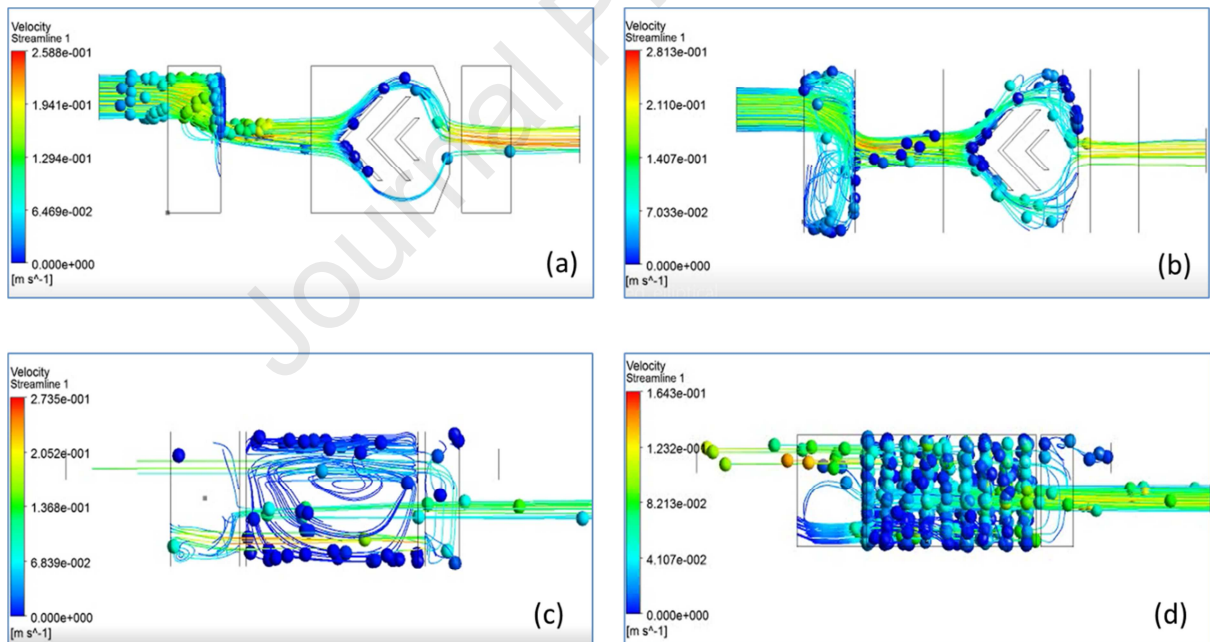


Fig.10 Velocity streamline from CFD simulation of: a: Type-A muffler, b: Type-B muffler, c: Type-C muffler and d: Type-D muffler

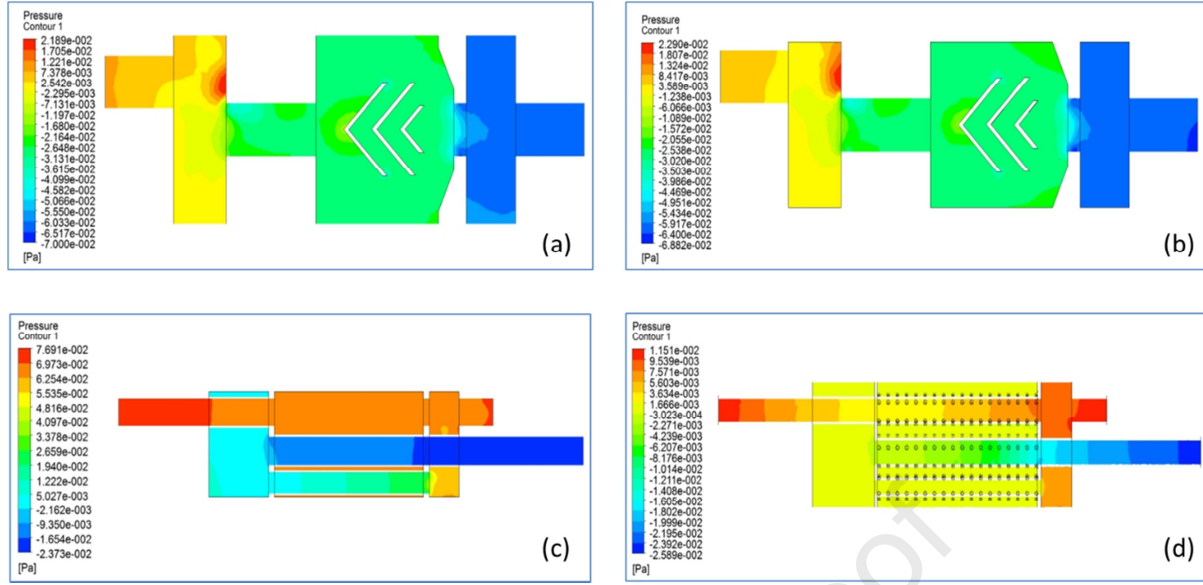


Fig.11 Backpressure from CFD simulation of: a: Type-A muffler, b: Type-B muffler, c: Type-C muffler and d: Type-D muffler

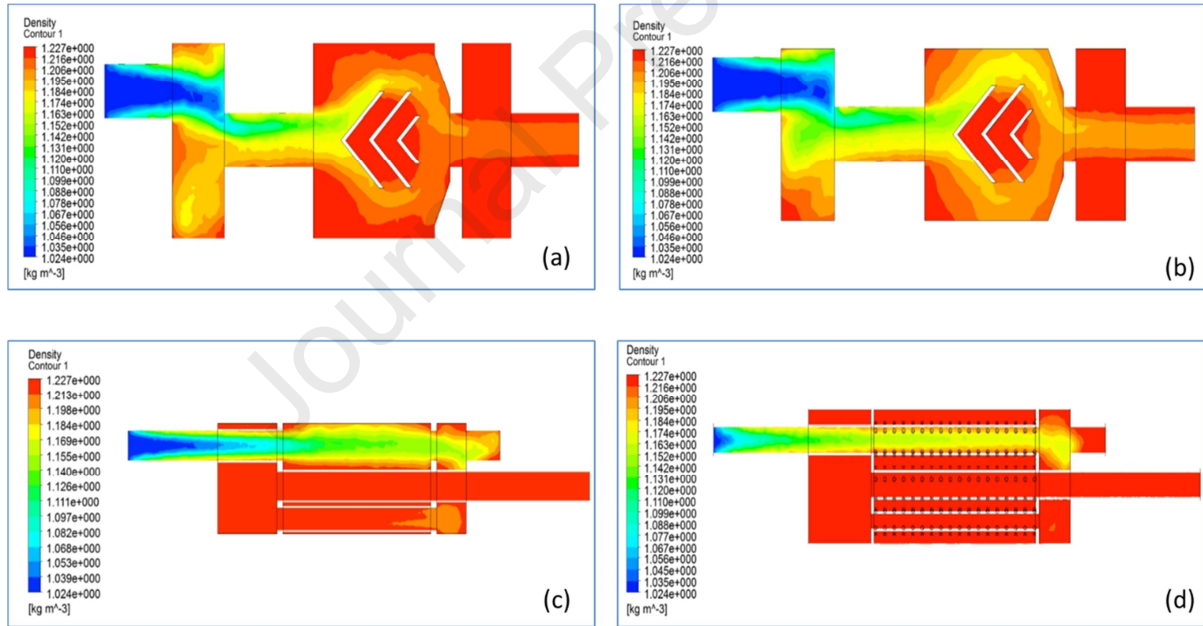


Fig.12 Emission gas density CFD simulation of: a: Type-A muffler, b: Type-B muffler, c: Type-C muffler and d: Type-D muffler

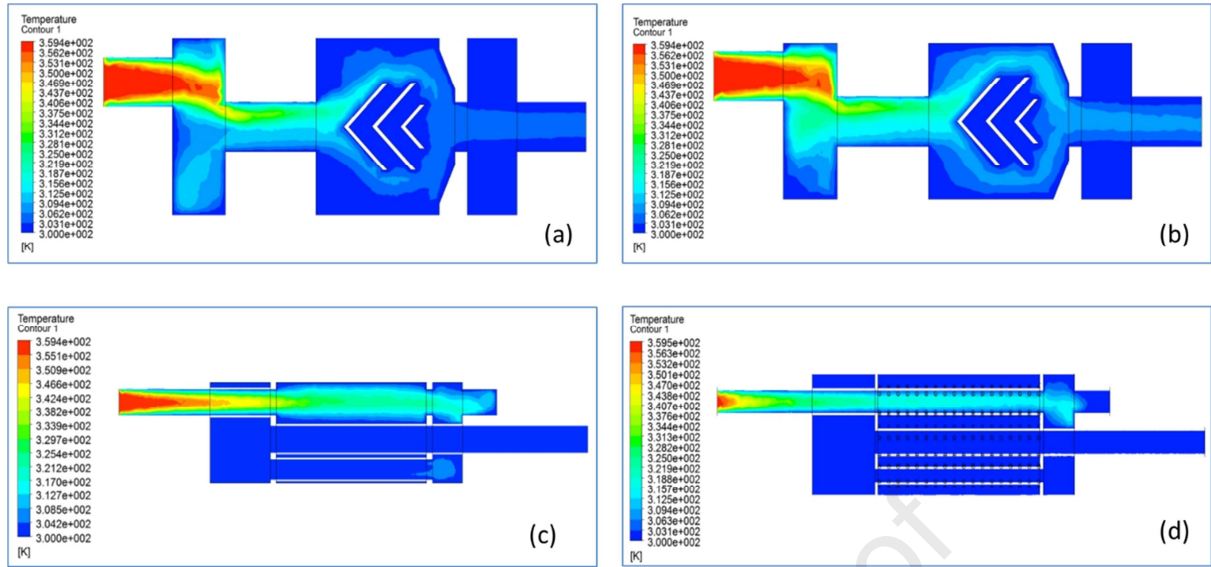


Fig.13 Emission gas temperature from CFD simulation of: a: Type-A muffler, b: Type-B muffler, c: Type-C muffler and d: Type-D muffler

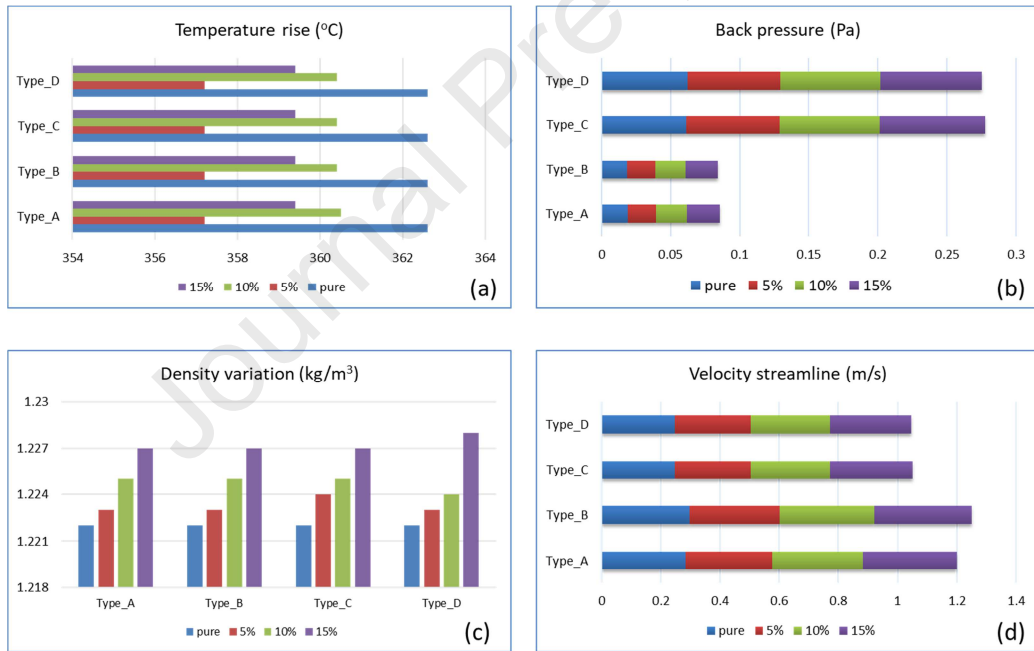


Fig.14 Bar chart of muffler performance, (a) Temperature rise, (b) back pressure variations, (c) density variation and (d) velocity stream line

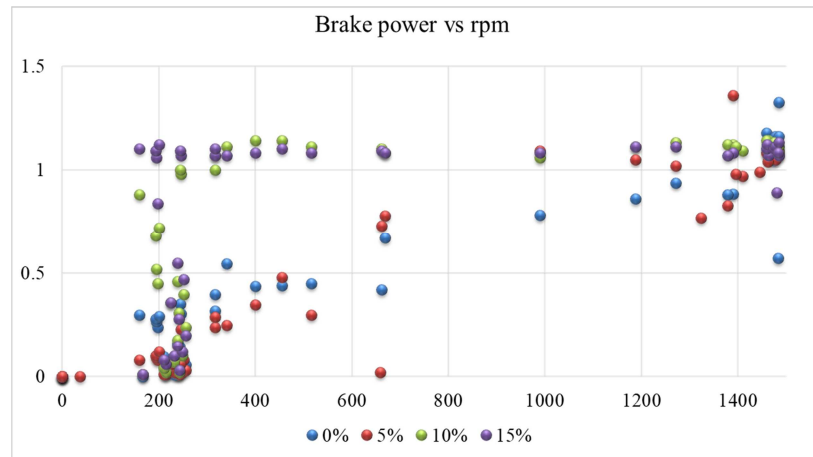


Fig.15 (a) Brake power response to rpm for different fuel replacement

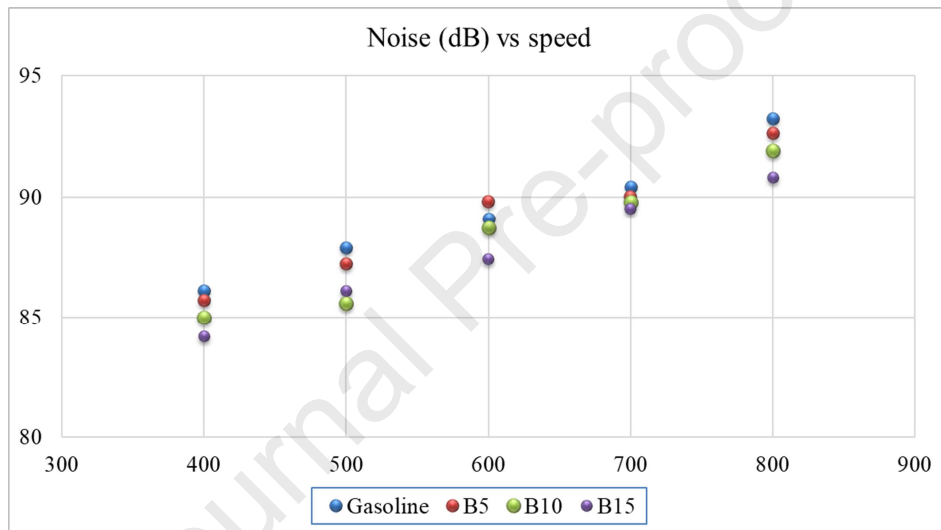


Fig.15 (b) Noise response to rpm for different fuel replacement

Research Highlights

Mitigation Strategy of Carbon Dioxide Emissions through Multiple Muffler design exchange and Gasoline-Methanol blend replacement

Research Highlights

- Need for blending Methanol-Gasoline to test and compare CO₂ emissions.
- Conduct Engine testing to carry out emissions and performance study.
- Mitigation strategy of CO₂ emissions through four-muffler design replacements.
- Sustainability of integrating fuel-blend and exhaust muffler design in CO₂ reduction.

Declaration of Competing Interest

We all authors declare that we have no known competing financial interests or personal relationships that could have appeared to influence the work reported in this paper.

Dr Prakash Chandra Mishra

Corresponding Author